REBUTTAL LETTER.

Antonio Manjón-Cabeza Córdoba and Maxim D. Ballmer, authors of the manuscript ‘The role of Edge-Driven Convection in the generation of volcanism I: a 2D systematic study’, thank the referees Prof. Jeroen van Hunen and Dr. Lisa Rummel for their thoughtful comments. All the comments are useful and, upon consideration, have allowed us to greatly improve the quality and content of the manuscript.

For the main changes of this version of the manuscript, we refer to the reply to the comments already submitted, for point-to-point responses, see below.

Reviewer 1:

Line 76: The model has no thermal boundary layer at its base, and therefore no convection is induced from below, only from lithospheric instabilities from above. This is likely to lead to long-term cooling of the model domain, which is unrealistic. Later on in the models, you apply increased levels of internal radiogenic heating, and find that some melting is indeed possible. I think such increased heating for the lack of convection due to absence of a bottom TBL. This approach was used in Kaislaniemi and van Hunen (2014). Perhaps this could be added to both justify the absence of a bottom TBL and the reasons for increasing internal heating rates.

The referee is correct in his assessment that our setting will lead to long-term cooling of the model, but these models are not intended to assess long-term evolution. We have added a few lines of discussion related to long-term radiogenic heating and model cooling (lines 305, 306 and 310-321).

Line 76: Is this with or without the adiabatic gracient of 0.3 K/km? Please make less ambiguous.

As per the referee’s request (and also following the advice of referee #2) we have changed these lines for clarification (lines 77-79).

Line 102: So depletion buoyancy and crustal buoyancy are lumped together in the same mechanism? With Delta rho_F = -100 kg/m3, this suggests that crustal buoyancy is only 100 kg/m3 for F=1. That is lower than the real buoyancy of crust. Perhaps this isn’t important, as all is needed is to have it buoyant enough to keep it floating. Please comment.

Yes, the reviewer is correct: we use the already existing buoyancy depletion to create a continental buoyant lid. It is also true that the density difference between the crust and the mantle is somewhat underscored using this approach. We clarify this in the text now (line 107). We also agree with the reviewer that, as long as the total (net) buoyancy (i.e., thermal+compositional) of the continental crust is positive, we do not expect any important caveats on the dynamics of the system, at least for the mid-term evolution (as is our focus here)..

At the beginning of this project, we actually ran test cases with a higher depletion value (~3) in the continental crust, but in a model setup without real topography, a very buoyant lid will create stresses that will tend to dissipate lateraly (Turcotte and Schubert, 2014) and may compromise the stability of (or the flow around) the edge. Thus, we abandoned this idea, now using a value of 1.0 as a compromise.

Line 102: Typo

We have corrected the typo.

Line 126: Can this be explained in a bit more detail?

We have expanded our explanation (now in lines 129-134).

Line 134: Throughout the manuscript, EDC and SSC are treated as separate phenomena, and indeed, they are. But the transition from one to the other is not always clear. Do you use a clear definition on what to call EDC and what SSC? I think it would be useful to add a sentence here that clearly defines these to modes of convection.

EDC is a type of SSC that is triggered by the presence of significant sublithospheric topography. The referee correctly points out that a 'clear distinction' between EDC and SSC can be confusing elsewhere in the paper. We have tried to reformulate the definition of EDC and SSC to make this clearer. We also clarify now how we distinguish SSC from EDC in terms of model analysis (lines 147-149).

Line 134: Given the rapid evolution of the LAB in this model, is the chosen initial condition compatible with the chosen model parameters? It seems that the chosen initial condition is not a realistic sustainable configuration.

We agree with the reviewer that the initial condition is not sustainable in the sense that the geometry of the edge remains stable over time (and the last timestep looks similar to the first). In this sense, the initial condition is metastable. However, there is hardly another approach to study this transient phenomenon, and all of the previous work has adopted a similar strategy of "imposing" an edge. In terms of the specific case of the Atlantic, EDC should have indeed already occurred somewhat earlier than timestep 0 of some of our models, and we discuss the implications of this in the manuscript (lines 289-296). We also note that we take great care to correctly simulate the initial thermochemical structure of the oceanic lithosphere, taking all relevant parameters into account to calculate the initial depletion profile (now more carefully described in the Appendix). In terms of the structure of the continental lithosphere, there are no such hard constraints, but we systematically explore continental thicknesses, and we have added an extended discussion about rheological stabilization in Appendix B. In terms of the edge, we explore width (*w*) independently of the other parameters (such as lithospheric thicknesses). In conclusion, we do not believe that the simplifications of our model affect our conclusions. To address this comment, we added some additional lines in the discussion for clarification (see lines 305-325).

Line 141: I understand the upwelling eroding the lithosphere locally. But can you elaborate on the stresses mentioned here? Do you mean local extension of the lithosphere?

We have realized that this sentence is confusing, and hence the comments by both reviewers. We therefore rephrase this section for clarity (see lines 151-154).

Indeed, "local extension of the lithosphere" is a more precise statement.

Line 143: Comparing the depleted lid thickness in Fig2 to the thermal thickness in Fig3 suggests that the base of the lithosphere is initially not depleted at all. So in order to achieve melting at the base of the lithosphere, is displacement of depletion by fertile material important, or just displacement of cold lithosphere by hot asthenosphere?

Due to our preliminary MOR models, melting does not occur along the adiabat unless depleted material is displaced. Displacement of depleted material is therefore essential, although this is also slightly dependent on the model.

We noticed, however, that we only show the field for peridotite in figure 2, and that this may lead to confusion since melting is mostly dominated by pyroxenite in most models. For clarity, we include a snapshot of the depletion of all lithologies in Appendix A. We also changed the colorscale in this figure to make small depletion values more visible.

Line 152: This analysis seems very reasonable to me for oceanic lithosphere. But we know that thick continental lithosphere is stable of very long timescales, which is not really featuring in your models.

Indeed, the base of the continental lithosphere develops SSC in our models, but we are not so sure that the bulk of the continental lithosphere is unstable on the timescale explored by our models. To further address this comment, we run a new suite of models with compositional rheology (lithosphere is further stabilized by accounting for the effects of dehydration stiffening) – see Appendix B.

Line 207: 7

We have corrected this typo.

Line 219: why is no oceanic age mentioned? Does the model really apply to the Canary Islands, given that lithosphere older than 50 Myr in your models leads to instabilities?

We do not mention the oceanic age because we keep it at the same value as in the reference case. For clarity, we have now added it to the text. According to our results, the oceanic crust beneath the Canary Islands must have suffered SSC for a long time. In any case, our main conclusion that EDC and/or SSC cannot account for volcanism at the Canaries remains robust. The predicted volumes of mantle melting are just too small for these mechanisms.

Line 284: our

We have corrected the typo.

Line 292: Mainly to compensate for a lack of basal heating due to large-scale mantle convection, see earlier comment.

We apologize if we have misunderstood the original intentions of Kaislaniemi and van Hunen (2014). We have rephrased this part for clarity in accordance with the referee's comment.

Reviewer 2:

Answers to the comments:

Line 70: Is there an effect of other discontinuities (e.g. at 410 km) as well? Do you include phase changes in your models?

We do not include the 410 olivine to ringwoodite reaction in our models. We base our choice in the widespread assumption that the 410 discontinuity is not an impediment to convection in general (if any, it may aid it). Technically speaking, melting is a phase change which we do include, but that is the only reaction that is present in the models.

Line 73: What would be the effect of a free surface as boundary? Do you emplace the extracted melt at the top?

We do not expect any relevant effect of changing the top or bottom boundary conditions, at least during the timespan of our models. We do not emplace extracted melt at the top: we do not expect this simplification to have a great effect, since degrees of melting are small, and the amounts of melt extraction are even smaller in all our models (in many cases: zero). We added 'outside the model box' in line 118 for clarity.

Line 77: What do you mean with "real temperature space"? Below the lithosphere?

We meant that, in reality, the bottom boundary condition becomes 1350 +0.3*660 C. We rephrased that line for clarity.

Line 81: Do you also include latent heat? Do you think it would have a big effect on the results?

Yes, the latent heat is included in the extended Boussinessq approximation (Christensen and Yuen, 85; see table 1). Yes, of course, it has a big effect. In fact, we believe that one of the reasons for overestimations of melting due to EDC in some of the previous work is the lack of consideration of latent heat.

Line 90: It would be nice to see a sketch showing the parameters w, To and Tc with varying geometries (maybe as zoom in Figure 2?)

The reviewer makes an excellent point. Unfortunately, τ makes reference to a time/age (which we cannot easily reflect on the figure 2); but we have added labels to each region in figure 2.

Line 90: maybe replace "," with "and" and add some words at the end: Hence, we systematically explore parameters age of the oceanic lithosphere (τo) and age of the continental lithosphere (τc) describing the different lithospheric thicknesses.

We rephrased this, and the next, sentence for clarity.

Line 94: Does this mean, that after melt extraction (depletion) it becomes more difficult to melt the residual? And if yes, how it is done? (see also comment Line 114)

Line 114: Do you emplace the melt somewhere after extraction? And do you deplete the material left behind after melt extraction? If yes, how? Is it dependent on the amount of extracted melt?

Yes, we include melt depletion of the residue after extraction. We follow the parameterization by Ballmer et al., 2009. In this parameterization, extracted melt acts as a 'permanent' F. This implies that new melting will not start until that F is reached and exceeded by the melting parameterization. For brevity, we have not included the whole approximation here, but we have rephrased some lines in these paragraphs for clarity. Regarding melt emplacement, see answer to comment of line 73.

Line 97: How F (depletion) is updated after melt extraction? Is after melt extraction (e.g. 10%) F increased by 0.1 locally on the marker?

That is correct, see our reply to previous comment. The details are provided in the cited literature (e.g., Ballmer et al., 2009).

Line 100-101: How you exactly construct your mid-ocean ridge model? You changed the geodynamic setting by keeping boundary conditions? Do you have extension? Do you then check what is the amount of melt that could be extracted leaving behind depleted residuals? How long do you run these models? Is the depletion constant for one age? How it is exactly done? Please add some Details! Maybe add a sketch.

We apologize for not being clearer in this regard. We have added a sketch and full explanations in Appendix A.

Because our objective is to evaluate melting under the conditions of our models, ridge models are simplified. Boundary conditions are different, with open bottom and right boundary to simulate a corner flow with lithosphere cooling on the top-left corner. Plate speed is imposed at the surface. Since we model only half of the ridge, 'extension' is implicitly imposed by these boundary conditions. Models are run until a statistical steady state is reached. The depletion profile is extracted from these models at a location sufficiently far away from the ridge axis (i.e., once melting ceases in a determinate column moving away from the ridge axis) at the steady state.

Line 102: Maybe change the sentence slightly:

For the initial depletion profile at the base of the continental lithosphere, we have chosen to impose the same ridge depletion as in the oceanic side and added additionally a depleted lid (with F = 1) on the top on the continental part (figure 2b)

Line 102: You use the depletion profile for the sub-crustal continental lithosphere right?

We slightly adjusted this sentence with some of the suggestions from the referee for clarity.

Line 104-105: Is the thickness of the lid the crust thickness? Adjusted for models with different continental lithospheric thickness? The crust follows the 0.9 Tref? If it is the lithosphere, then maybe replace "to" with "that". How the crust thickness changes with changing lithospheric thickness?

This lid refers to the 'crust-like' lid, correct. We rephrased this sentence for clarity. Below the lid, the depletion is fixed by the preliminary ridge models, the only free parameter we can adjust is the continental 'lid' thickness. As the lid thickness is changed, the depth of the 0.9 * T_{ref} isotherm is adjusted accordingly (through modification of τ_c).

Figure 2: Can you label it? Where is the LAB (maybe isolines)? Where is crust and continent, the edge?

We added the labels from comment to line 90. Since the geodynamic LAB is not well defined, we believe that the inclusion of isotherms in this figure will make it more difficult to read, and perhaps even misleading.

Line 112: Is the only difference between depleted and enriched peridotite the water content?

That is correct. Since we do not track melt composition in our models, we believe that this approximation is valid. This approach follows the work by Ito and Mahoney (2005), Bianco et al. (2008), and Ballmer et al. (2009).

Line 111-113: Is the total melt averaged from the different laws?

The amount of melt from the different lithologies is indeed pooled (see line 114). We assume that the melts efficiently mix with each other in the mantle or a shallow magma chamber.

Line 125: Why it is important that the slope of the viscosity profile along adiabat remains the same?

There are two main reasons for this. The first is the approximation to viscosity from equation (2), that induces a non-physical double dependency of the viscosity. The Second is our approximation to 'dislocation-creep-like' rheology of line 121, which force us to explore the effect of the activation energy in an independent way from activation volume.

We understand that this was not sufficiently clear, so we added some clarification (lines 129-134).

Table 1: What is with phi used in equation 1, maybe list it as well? In the table latent heat is mentioned, in which equation this parameter is included? Are the values in front of the brackets always the reference values? If yes, please say this in the caption.

φ is not a model parameter; it is a field variable (such as temperature or viscosity). Latent heat is in the energy conservation equation according to the extended Boussinessq approximation (Christensen and Yuen, 1985; also see Ballmer, 2009). We included the requested clarification in the caption.

Line 129: Maybe add a small introduction in that paragraph.

We added a line for clarity.

Figure 3: Maybe add important values that you have changed for other models then it could be easier for the reader to compare the figures (e.g. Ea and viscosity) (also for Figure 4). Maybe describe also the meaning of the arrows. Maybe it would be also nice to see other plots than temperature, for example different rock types/depletion stages and how they are mixed with time.

Since many parameters are changed in the models here presented, adding all relevant parameters would make this caption illegible, we prefer to refer the reader to table 1. Nonetheless, we added the parameters of the reference case to figures 4 and 7 for a better comparison. In addition, we added a line in the caption clarifying that the arrows represent the velocity field. We also added the requested depletion field in Appendix A.

Line 141: Why stresses induce the bumb?

Every gradient in velocity imply stress, it is another way of saying that the upwelling interaction with the base of the lithosphere, in addition from material entrained in the downwelling, causes the bump.

We have rephrased this sentence, because it was a problem for both reviewers.

Line 143-145: What do you mean? You have to shift material below the base of the lithosphere to induce melting? Because you have to increase the temperature of lithospheric material to exceed the solidus curve?

We rephrased these lines for clarity (as a response to this comment, but also as a response to a comment by reviewer 1).

Line 154: Maybe write: Figure 4b

That is a good catch, we apologize for the inconsistency.

Figure 5a: typo: Pa s

We corrected the typo.

Figure 6: typo in (b): Pyroxenite/Total. First line: reference viscosity (typo?); Point is missing at the end of caption; Why z = 206 km is used, please clarify;

We corrected the typos. We use the viscosity at 206 km because it represents the viscosity of the asthenosphere. This value is more relevant to most readers than the reference viscosity, which only makes sense in the context of equation 2, but does not necessarily represent the viscosity of a specific region of the mantle. Adding this full explanation in the caption would make the caption too long, so we have added a line in the main text for clarity (line 193).

Lines: 191-193: You define the amount of enrichment only the amount of pyroxenite melting, right? Or is the amount of melt considered as well? Do you track the chemistry of melt?

The referee is correct, we only check the amount of pyroxenite melting **with respect** to total melting. We are not sure what the referee means by 'chemistry' of the melt, but we do not track major-element composition, nor trace-element composition.

Line 222: why SSC = 48+40 Myr? Why +40?

We apologize for this mistake. In an earlier version of the paper, we included +40 in all ages for SSC start (also in the axes of figure 5) because the models start at 40 Ma. After careful consideration, we decided to eliminate this notation but forgot to correct it in this line.

Line 249: typo? from 15 % to 25 %?

We have corrected the typo.

Line 278-280: Which of your results are then realistic and which not? Is the EDC seen in your models sometimes just an artefact because of the metastable conditions at the beginning? Would it be then not better to start with a middle ocean ridge next to a continent to see the real evolution?

We refer the reviewer to our answer to the comment about line 134 of reviewer #1.

Line 341-342: Maybe the paper of Tobias Keller could be interesting: Keller, T. , Katz, R. F. and Hirschmann, M. M. (2017) Volatiles beneath mid-ocean ridges: deep melting, channelised transport, focusing, and metasomatism. Earth and Planetary Science Letters, 464, pp. 55-68. (doi:10.1016/j.epsl.2017.02.006).

We appreciate the suggestion by the referee. Unfortunately, the Keller *et al.* approximation is not consistent with our treatment of water (and their treatment of water is not necessarily more accurate than ours, albeit being more precise), and it requires a complete reformulation of the constitutive equations. These equations (in Keller et al.), in turn, are suitable for close-to-steady state models that can be evaluated in a near-instantaneous fashion, but they are not suitable for our models (*i.e.* wide parameter space with models that span several millions of years).

Line 387: I would add “low” (e.g. low Ea and/or low eta0)

Corrected.

Line 83 and Line 220, 339: maybe delete “,” before “;” in the citation

We corrected these typos.

Line 125: typo: we slightly

Line 284: typo: many of our results

Maybe it is better to use always our and we instead of my and I: **Line: 287, 293, 303, 345, 352, 353, 368**

We apologize for this repeated typo. In an earlier version, this paper was written in first person. We corrected these mistakes.

Line 206: typo: Figure 7

We fixed this typo.

Line 260: typo: H2O

We fixed this typo.

Line 318: typo: with a spacing

We fixed this typo.

Line 394: typo: replace "." with ","

We fixed this typo (although we did it by capitalizing 'W').

The role of Edge-Driven Convection in the generation of volcanism I: a 2D systematic study

Antonio Manjón-Cabeza Córdoba[1] and Maxim Ballmer[2,1]

[1]ETH Zürich, Department of Earth Sciences, Institute of Geophysics
[2]University College London, Department of Earth Sciences

Correspondence: Antonio Manjón-Cabeza Córdoba (antonio.manjon@erdw.ethz.ch)

Abstract. The origin of intraplate volcanism is not explained by the plate tectonic theory, and several models have been put forward for explanation. One of these models involves Edge-Driven Convection (EDC), in which cold and thick continental lithosphere is juxtaposed to warm and thin oceanic lithosphere to trigger convective instability. To test whether EDC can produce long-lived high-volume magmatism, we run numerical models of EDC for a wide range of mantle properties and edge (*i.e.*, the oceanic-continental transition) geometries. We find that the most important parameters that govern EDC are the rheological paramaters parameters mantle viscosity η_0 and activation energy E_a. However, even the maximum melting volumes found in our models predicted by our most extreme cases are insufficient to account for island-building volcanism on old seafloor, such as at the Canary Islands and Cape Verde. Also, beneath old seafloor, localized EDC-related melting commonly transitions into widespread melting due to small-scale sublithospheric convection, inconsistent with the distribution of volcanism at these volcanic volcano chains. In turn, EDC is a good candidate to sustain the formation of small seamounts on young seafloor, as it is a highly transient phenomenon that occurs in all our models soon after initiation. In a companion paper, we investigate the implications of interaction of EDC with mantle-plume activity.

1 Introduction

Understanding the origin of volcanism improves our understanding of Earth's deep interior processes, structure and composition. In this context, intraplate volcanism deserves particular attention, because it is not readily explained by plate-tectonics processes. One of the leading theories to explain intraplate magmatism involves mantle plume theory. In this theory, a magmatic hotspot is sustained by a fixed and columnar mantle upwelling, or "plume", forming a volcano chain on a steadily moving plate (Wilson, 1963; Morgan, 1971).

Plume theory makes specific testable predictions, such as the distribution of volcanism, the age-distance relationship along the volcanic chain, as well as anomalies in heat-flux and topography (hotspot swells). These predictions have been successfully compared to observations at several locations (*e.g.* Hawaii, Louisville…), however, comparisons fail at other locations (see

Courtillot et al., 2003). For example, the age-distance relationship measured along the Pukapuka Ridge does not agree with the overriding plate motion (Sandwell et al., 1995; Ballmer et al., 2013); at Madeira, there is no apparent swell (Anderson, 2005; Ballmer et al., 2013; King and Adam, 2014); etc. Accordingly, alternative or complementary models have been proposed for sustaining intraplate volcanism (Foulger and Anderson, 2005; Hirano, 2011; Ballmer et al., 2015; Green, 2015).

One of these models involves Edge-Driven Convection (EDC; King and Anderson, 1995, 1998). EDC is a variant of small-scale convection (SSC; Richter, 1973; Parsons and McKenzie, 1978; Huang et al., 2003; Dumoulin et al., 2005), *i.e.* a thermal boundary-layer instability that is largely driven by cooling of the lithosphere and the related density inversion (Ballmer et al., 2009; Ballmer, 2017). EDC is triggered by the presence of lithospheric steps (or lateral heterogeneity): the related lateral density difference promotes the instability (which is ultimately driven by the density inversion), setting up a convection cell (figure 1). But apart from this, it has all the characteristics of SSC. According to King and Anderson (1995, 1998), the associated upwelling(s) may be sufficient to sustain mantle melting without the need of a plume. This magmatism is predicted to occur at a distance from the step in lithospheric thickness (*e.g.*, nearby a cratonic margin) of a few hundred kilometers.

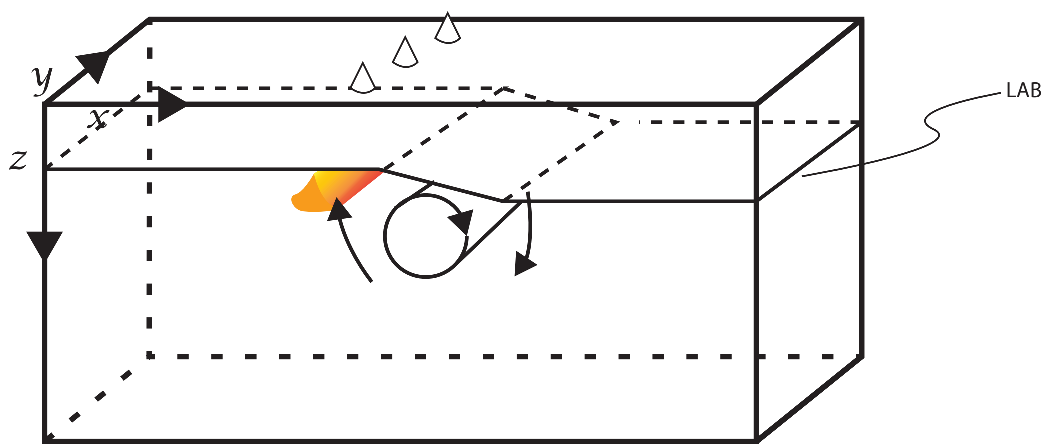

Figure 1. Schematic of Edge-Driven Convection. A downwelling is promoted on the thick continental side of the lithospheric edge, triggering a passive upwelling that sustains mantle decompression melting (orange) and related volcanism parallel to the continent-ocean transition (cones). The Lithosphere-Asthenosphere Boundary (LAB) is labeled.

In the Atlantic Ocean basin, several volcanic chains occur near the margin of the continental platform (*e.g.*, the Canary Islands, Cape Verde or the Cameroon Volcanic Line). For many (or all) of these chains, several predictions of classic plume theory are not fulfilled. For example, the Canary Islands do not display a strictly linear age progression, with coeval volcanism occurring over hundreds of kilometers and sustained volcanism at a single island or seamount for >20 Ma (Abdel-Monem et al., 1971, 1972; Carracedo, 1999; Geldmacher et al., 2005). Given these complexities, several alternative hypotheses have been proposed. For instance, some authors have invoked the extraction of magmas along elongated shear zones of preexisting melt (Araña and Ortiz, 1991; Doblas et al., 2007; Martinez-Arevalo et al., 2013), possibly associated with a thermal anomaly (Anguita and Hernán, 2000)(Anguita and Hernan, 2000). Alternatively, the "passive" upwelling of "mantle blobs" (Hoernle and Schmincke, 1993; Thirlwall et al., 2000), or EDC with or without a contribution from a nearby plume (King and Ritsema, 2000; Geldmacher et al., 2005) may sustain Canary volcanism. EDC has also been proposed as an underlying mechanism for other Atlantic hotspots such as Bermuda or Cape Verde (Vogt, 1991; King and Ritsema, 2000).

Despite the long-lasting debate on the origin of near-continental intraplate volcanism, there is no published comprehensive geodynamic study of EDC and related magmatism in a continental-oceanic setting. Some authors (King and Ritsema, 2000; Sacek, 2017) have explored the dynamics of this mechanism, and applied their results to the eastern Atlantic, but have not explicitly and consistently modeled mantle melting. Others have studied EDC in great detail but for a purely continental setting (van Wijk et al., 2008, 2010; Till et al., 2010; Kaislaniemi and Van Hunen, 2014; Ballmer et al., 2015; Currie and van Wijk, 2016).

In this contribution, we study EDC-related flow and melting in the upper mantle using numerical models in order to understand the origin of intraplate volcanism in the eastern Atlantic. EDC can be approximated as a purely two-dimensional (2D) mode of convection, with convection roll(s) infinitely extending along the continental margin (King and Anderson, 1995; Kaislaniemi and Van Hunen, 2014). Therefore, we have chosen to investigate 2D models, which allows us to explore a wide parameter space, and to test the potential of EDC to systematically sustain intraplate volcanism. Finally, we compare model predictions with observations at the Canaries and Cape Verde and evaluate the limitations of our results in the limit of our model assumptions.

We find that melt generation by EDC alone is too restrictive and transient to be a suitable explanation for the occurrence of large volcano chains such as the Canary Islands or Cape Verde. Our models predict that EDC *sensu stricto* generates volcanism only for a small subset of the parameter space, and if it does so, only with small amounts of very enriched volcanism, and only below young and thin oceanic lithosphere. EDC remains a suitable explanation for small seamounts in the area (*e.g.* Van Den Bogaard, 2013). A companion paper (citationcomplementary paper (to be submitted) explores the dynamics of plume-EDC interaction, showing that a contribution from at least a weak plume is required to sustain island-building volcanism.

2 Methods

We run 2D numerical models using the mantle-convection code CITCOM (Moresi and Solomatov, 1995; Moresi and Gurnis, 1996; Zhong et al., 2000) with the additions described in Ballmer (2009). We use the code to solve the equations of conservation of mass, momentum and energy according to the “extended Boussinesq approximation” (Christensen and Yuen, 1985) in a Cartesian frame of reference. Non-diffusive fields (*e.g.* composition or melt depletion) are advected by passive tracers. King and Ritsema (2000) demonstrate that EDC is confined to the upper mantle whenever the phase change at 660 km is present, so all our experiments are regional models with a vertical extent of 660 km. The Cartesian model box of dimensions 2640x660 km is resolved by 384x96 elements without grid refinement. Resolution tests confirm that results converge well at this resolution.

Kinematic boundary conditions involve no slip at the top and bottom boundaries. In some models, a non-zero plate velocity (v_{plate}) is imposed. When v_{plate} is 0, both side boundaries are free slip. Otherwise, we impose a self-consistent (Couette-like) velocity profile in the inflow (left) boundary and open the opposite outflow boundary.

In terms of thermal boundary conditions, we impose potential temperatures of T_{surf} = 0 °C and T_{ref} = 1350 °C at the top and bottom, respectively. In real temperature space, These temperatures are potential in nature, and therefore do not take into account any possible adiabatic gradient. When doing any calculation that would need a more realistic temperature (*e.g.* viscosity, melting), an adiabatic gradient of 0.3 K·km^{-1} is added (*i.e.*, the bottom temperature corresponds to 1350 + 0.3 $*$ 660 = 1548 °C). Lateral boundaries are reflective (zero heat flow) except when inflow happens because of finite plate motion, in which case the thermal boundary condition is fixed at the initial profile. The models also include internal (*i.e.*, radioactive) heating with a reference value of H = 7.75·10^{-12} W·kg^{-1}, but we also run models with higher values of H. In addition, we discuss models with increased radiogenic heating that occurs only in the continental crust.

The initial thermal profiles of the oceanic (left) and continental (right side of the box) lithosphere are calculated according to the half-space cooling model (*e.g.* Turcotte and Schubert, 2014, ; figure 2a) (*e.g.* Turcotte and Schubert, 2014, figure 2a) plus a small random thermal noise to simulate small-scale heterogeneity and advance the solution of the initial timesteps. Both the thermal age of the continental lithosphere and the age of the oceanic lithosphere are free model parameters (τ_c, τ_o). The edge (*i.e.*, the transition in lithospheric thickness) is imposed as a linear interpolation between the oceanic and continental lithospheric thermal profiles. We chose choose this setting because it allows us to freely vary the geometry of the transition between oceanic and continental lithosphere.

The geometry of the edge is an unconstrained parameter, the effects of which on EDC have not yet been studied systematically. The edge is defined by the initial lithospheric thickness on either side, and the width of the linear transition between the two (w). Hence, we systematically explore parameters age of the oceanic lithosphere (τ_o), age of the continental lithosphere (τ_c). To study how much the dynamics change due to a change in the aspect ratio of the transition between ocean and continent, we also changed the width of the wedge between the two lithospheres (w).

The modeled mantle consists of a fine-scale mixture of peridotite (97 %) and recycled basaltic eclogite (3 %, from now on, pyroxenite; Hirschmann and Stolper, 1996). Mantle depletion of both lithologies increase with increasing degrees of melting, which affects mantle density ρ:

$$\rho = \rho_{ref} - \alpha \cdot \rho_{ref} \cdot (T - T_{ref}) + F \cdot \Delta\rho_F + \phi \cdot \Delta\rho_\phi \tag{1}$$

where ρ_{ref} is the mantle density at T_{ref}, α the thermal expansivity, T the temperature, F the melt depletion extent, ϕ the mantle porosity, and $\Delta\rho_F$ and $\Delta\rho_\phi$ the density differences related to melt depletion and melt retention (Schutt and Lesher, 2006; Ballmer et al., 2009). The depleted lithosphere is, therefore, more buoyant than the underlying mantle. To calculate the initial depletion profile of the oceanic lithosphere for our EDC models, we run 2D simulations of flow and melting of a simplified mid-ocean ridge using the same parameters as in the corresponding EDC models. An example of one of these ridge models can be found in appendix A

As for the initial depletion profile at the base of the continental lithosphere, we have chosen to impose the same ridge depletion as in the oceanic side on the continental part, adding a depleted lid (with F = 1) on the top (figure 2b). This depleted lid mimics the excess buoyancy of continental crust, although it may underestimate the actual density values of the upper crust. The initial thickness of this lid is arbitrarily defined as 40 km for the reference case, but it is adjusted for models with different continental thicknesses to follow the $0.9{\cdot}T_{ref}$ isotherm on the continental side. The edge itself consists on a wedge of crustal depletion (F = 1) of width w that thins toward the oceanic lithosphere (figure 2). Indeed, it has been suggested that the subcontinental lithospheric mantle is harzburgitic in nature (Bodinier and Godard, 2013), but the specific profile remains unconstrained.

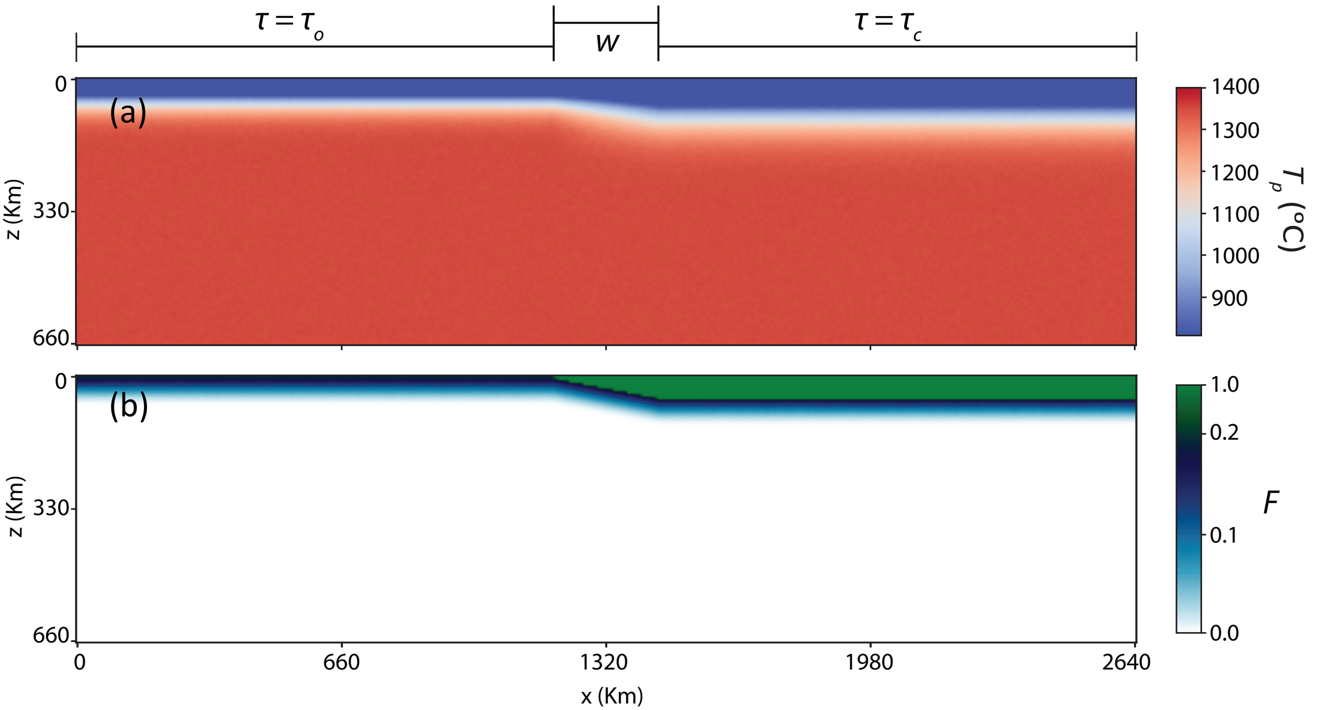

Figure 2. Initial conditions for the reference model. (a) Initial field of potential temperature T_p (*i.e.* with the adiabatic gradient removed). (b) Initial compositional field of depletion (F) for the hydrous peridotite component. The areas where $\tau = \tau_o$ and $\tau = \tau_c$, as well as w, are labeled for clarity. A comparison of the fields for different lithologies can be found in Appendix A (figure A2).

We consider melting explicitly in our models following Ballmer et al. (2009), assuming that the lithological assemblage consists of 82% depleted peridotite, 15% enriched peridotite (for the aforementioned sum of 97%) and 3% pyroxenite. Peridotite melting is calculated using the parameterization of Katz et al. (2003). We impose an H_2O content of 100 ppm for the background depleted peridotitic component, and 300 ppm for the enriched peridotitic component (H_2O is a placeholder for any kind of enrichment). The pyroxenite melting law is taken from Pertermann and Hirschmann (2003). Melt flow and extraction occurs on timescales much shorter than convective flow. We therefore assume instantaneous extraction (outside the model box) of any melt fractions that exceed the critical porosity (ϕ_c).

We use a simplified rheology with a dependence of viscosity on temperature T and pressure P:

$$\log\eta = \log\eta_0 + \frac{E_a + P\cdot V_a}{R\cdot T} - \frac{E_a}{R\cdot T_{ref}} \tag{2}$$

where η is the viscosity, E_a and V_a the activation energy and volume, respectively, T and P are the temperature and pressure, R the ideal gas constant and T_{ref} is the reference (potential) temperature. In this formulation, η_0 is the reference viscosity defined at $T = T_{ref}$ and zero pressure, and hence does not represent the viscosity of the asthenosphere. Our reference activation energy is 200 kJ $\cdot$ mol^{-1}, *i.e.*, lower than the lower limit constrained by deformation experiments (Karato and Wu, 1993; Hirth and Kohlstedt, 1996). We use such reduced values for E_a to account for the effects of stress-dependent viscosity (*e.g.*, due to dislocation creep) in a simplified Newtonian rheology description (Christensen, 1984; van Hunen et al., 2005). We do not consider the effects of compositional (*e.g.* pyroxenite vs. peridotite, water-dependent) rheology in this work.

Our choice of the rheology parameterization causes the true depth-dependency of viscosity to be due to both, E_a and V_a (eq. 2). This dependency is problematic because, due to the simplified parameterization and our decreased E_a, the effect of the physical parameters on the viscosity along the adiabat is unrealistic. Instead, we chose to keep the viscosity along the adiabat constant and chose to focus on the effect of E_a on the stability of the Lithosphere-Astenosphere Boundary, which is crucial for any kind of SSC (including EDC). To make sure that the slope of the viscosity profile along the adiabat remains the same in all cases, We we slightly adjust V_a as parameter E_a is varied. Any variations in V_a (see table 1) are only due to this adjustment.

3 Results

3.1 Reference case

To characterize flow and melting of EDC, we first describe a reference case. Figure 3 shows a typical example of EDC as a series of snapshots for the reference case. The convective pattern initially resembles (figure 3a) the pattern of the idealized case in figure 1, as well as the cases reported by King and Anderson (1998): there is one major convection cell with a dominant downwelling on the continental side of the edge and upwelling return flow on the oceanic side. The downwelling is mainly sustained by lateral inflow of sub-lithospheric material from the oceanic side due to the asymmetry in viscosity structure, but some material from the continental side is also entrained. As a response to this entrainment, a secondary return-flow upwelling is soon generated on the continental side (figure 3b). The flow patterns, however, promptly change to more complex configurations, with several upwellings and downwellings adjacent to the initial convection cell. Soon thereafter (at 35∼40 Myr), the oceanic lithosphere as a whole becomes thermally unstable triggering widespread small-scale convection (SSC; figure 3d). At this point, EDC becomes almost undistinguishable from SSC (in our 2D models).

From this point, we do not characterize EDC further, as it is not possible to distinguish which properties are due to EDC and which ones are due to SSC. We therefore define this onset of SSC as the maximum of the first time-derivative of the second peak of the $v_{z,rms}$ (the first peak corresponds to EDC).

Table 1. Relevant reference parameters for the models described in this chapter. Values between parenthesis represent the explored parameter space, with the exception of V_a (see section 2 for explanation)

Notation	Parameter	Value(Range)	Unit
T_{ref}	Reference temperature	1350 (1300-1400)	°C
D	Reference thickness	660	km
ρ_{ref}	Reference density	3300	kg·m^{-3}
κ	Thermal diffusivity	1·10^{-6}	m^2·s^{-1}
g	Gravity acceleration	9.8	m·s^{-2}
α	Thermal expansivity	3·10^{-5}	K^{-1}
c_P	Heat capacity (constant pressure)	1250	J·kg^{-1}·K^{-1}
η_0	Reference viscosity	8.61·10^{18} (2.87·10^{18}-1.96·10^{19})	Pa·s
E_a	Activation energy	200 (120-300)	kJ·mol^{-}1
V_a	Activation volume	5.00·10^{-6} (4.54·10^{-6}-5.82·10^{-6})	m^3·mol^{-1}
γ_a	Adiabatic gradient	0.3	K·km^{-1}
H	Internal heating	7.75·10^{-12} (7.75·10^{-12}-2.33·10^{-11})	W·kg^{-1}
F	Melt depletion	0-1	-
$\Delta\rho_F$	Density anomaly due to melt depletion	-100	kg·m^{-3}
ϕ_c	Critical porosity	0.01	-
$\Delta\rho_\phi$	density anomaly due to melt retention	-100	kg·m^{-3}
L	Latent heat of melt	5.6·10^5	J·kg^{-1}
v_{plate}	Plate velocity	0-6	cm·yr^{-1}
τ_c	Age of the continental lithosphere	100(70-300)	Ma
τ_o	Age of the oceanic lithosphere	40(30-50)	Ma
w	Width of the edge	264(132-396)	km

Ultimately, SSC also develops beneath the continental lithosphere (~45 Myr, not shown).

An important consequence of EDC (and subsequent SSC) is the erosion of the base of the lithosphere (represented by the black contour in figure 3). At 21 Myr (figure 3b), a clear 'bump' (or small cavity; Conrad et al., 2010) appears at the base of the lithosphere due to the stresses that are imposed by the upwelling upwelling pushing the material, as well as material entrainment by the major downwelling, hence promoting local extension of thelithosphere. Not only is this thermal erosion partly responsible for triggering secondary downwellings and transmitting SSC toward the oceanic side (figures 3c,d) (*e.g.* Dumoulin et al., 2005), but it is also a requirement for melting. Displacement of at least the base of the depleted lid is necessary for melting, because

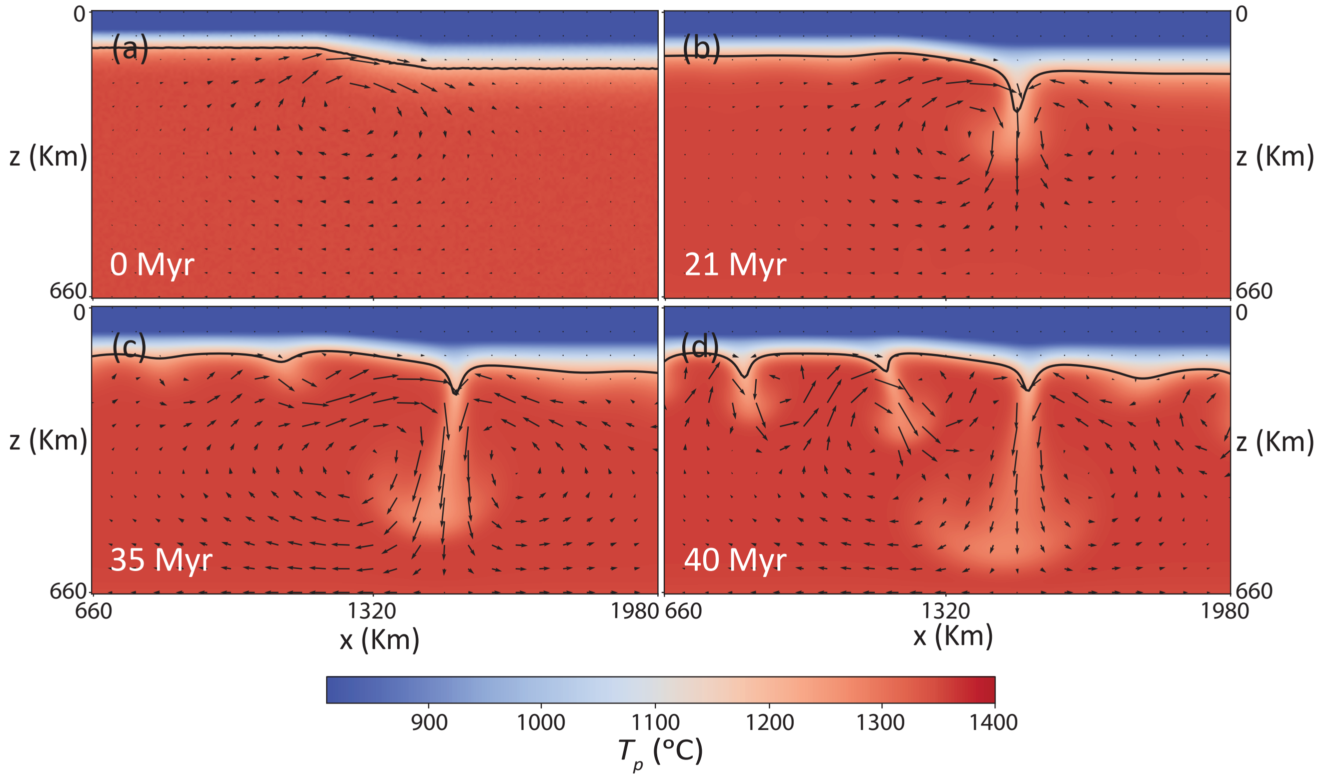

Figure 3. Series of snapshots of potential temperature for the reference case (for parameters, see table 1). In black, the 1215 °C isotherm ($0.9{\cdot}T_{ref}$) is shown as a proxy for the base of the lithosphere. Arrows reflect the instantaneous velocity field. No melting is predicted by this model at any timestep.

the temperatures are below the melting point of the lithosphere at timestep zero. Nonetheless, in this reference model, erosion of the depleted lid remains insufficient to allow mantle melting to occur throughout model evolution.

3.2 Effects of physical properties of the mantle

To understand the optimal conditions for melting generated by Edge-Driven Convection, we systematically explore several physical properties of the models. We focus on the effects of reference viscosity (η_0), activation energy (E_a) and initial potential temperature (T_{ref}).

Increasing the reference viscosity (according to eq. 2) tends to delay the onset of convective instability and hamper melting (figures 4a,b; 5a). Thereby, the duration of EDC (which starts immediately at t = 0, albeit with a smaller vigor compared to the reference case) vs. SSC is enhanced. Figure 4 (b) shows a snapshot of a case with η_0 = $1.95{\cdot}10^{19}$ Pa·s, which displays a similar pattern of convection as the reference case with η_0 = $8.61{\cdot}10^{18}$ Pa·s (figure 3c), but at a much later model time of 82

Myr. Accordingly, the onset of SSC is much later than estimated for a typical ocean basin on Earth (Stein and Stein, 1994; Doin and Fleitout, 1996), and the lithospheric thickness on the oceanic side of the model is far too thick to potentially allow the astenosphere to melt. In turn, cases with $\eta_0 \leq 3.83{\cdot}10^{18}$ Pa·s (figures 4c, 5a) display melting during a limited period of time (*i.e.*, over a few Myr), but based on the (late) timing and (widespread) distribution of melting, most of this melting is associated with SSC rather than with EDC (see figure 4c).

Decreasing activation energy (figures. 4c, 5b) tends to advance and increase the vigor of EDC and SSC. For low E_a, the viscosity of the base of the lithosphere is decreased, and hence the lithosphere becomes more mobile. For $E_a \leq 140$ kJ·mol^{-1}, the related erosion of the base of the lithosphere is sufficient to permit early and localized EDC-related melting. However, in these cases, more vigorous melting ultimately occurs across the entire oceanic domain due to SSC. Also, the onset of SSC and related seafloor flattening is < 70 Myr, *i.e.*, earlier than realistic for the Atlantic (Stein and Stein, 1994), although we can compensate this by choosing a different reference viscosity. In turn, cases with high $E_a \geq 250$ kJ·mol^{-1} display a late onset of SSC and a stable lithosphere with ultimate thicknesses greater than realistic (figures 4d, 5b).

Regarding convection patterns, the entrainment of sublithospheric material by the dominant downwelling near the edge tends to be more symmetric for low E_a. This prediction implies that that the activation energy will have an important effect on the final geometry of the oceanic-continental transition. Finally, cooling of the mantle is more efficient for low E_a than for high E_a, since the base of the lithosphere is more mobile. This effect also occurs for decreasing η_0, but is more pronounced for decreasing E_a (see isotherms in figure 4a vs. figure 4c).

Increasing T_{ref} tends to advance convective instability and boost magmatism. An increment of potential temperature from 1350 °C to 1400 °C (figure 4e) induces minor melting in the area of maximum erosion of the lithosphere during a limited period of time. This effect is smaller than expected because it is largely compensated by an increase of the thickness of the pre-calculated depleted lithosphere (see section 2), and because the lithosphere still cools via conduction. Increasing the temperature even more may further increase melting, but would also lead to unrealistic crustal thicknesses in the corresponding pre-calculated models. Also note that the peridotite melting parameterization used in this study (Katz et al., 2003) is on the lower end in terms of solidus temperatures (*e.g.* McKenzie and Bickle, 1989; Iwamori et al., 1995; Hirschmann, 2000; Lambart et al., 2016).

Figure 6 presents a summary of the joint effect of η_0 and E_a on EDC-related mantle melting. We also label the viscosity at 206 km depth as a representative of the viscosity of the asthenosphere. The melting rate characteristic for EDC (figure 6a) is determined at the first local maximum of root-mean square vertical velocity $v_{z,rms}$, which corresponds to the development of the first major downwelling from near the edge. Determining the exact volume of EDC-related melting remains difficult because melting occurs before and/or after this maximum, and commonly transitions into persistent SSC-related melting. For example, the model with E_a = 140 kJ·mol^{-1} (and with reference values of η_0) displays some EDC-related melting just before the onset of SSC, but this melting episode is extremely short-lived and would likely be insufficient to sustain any significant volcanism. Nonetheless, there is a systematic trend between melt volume fluxes that are measured as described above with both parameters. This result suggests that the stability and final thickness of the lithosphere ultimately controls melting due to

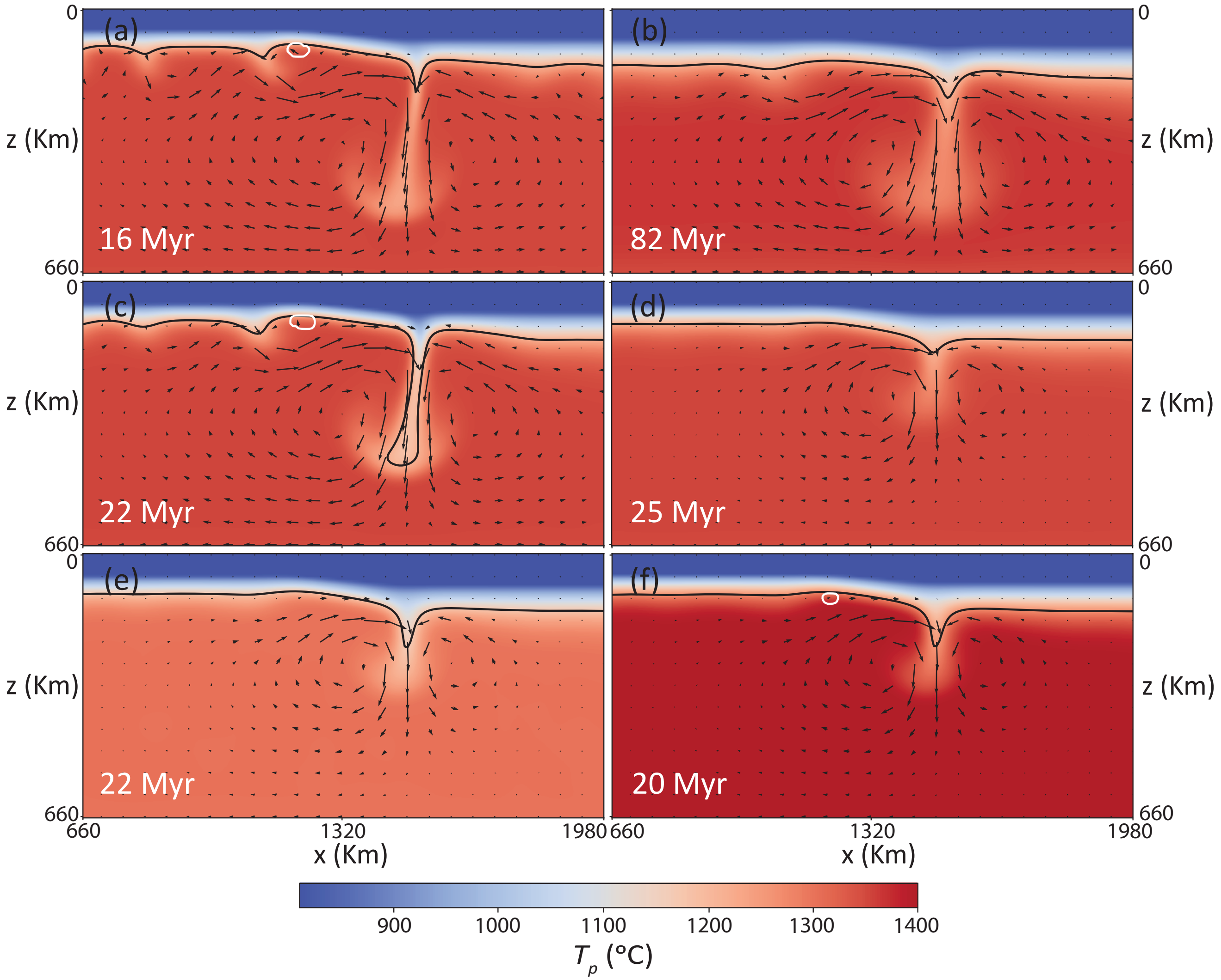

Figure 4. Effects of rheological parameters and reference temperature on Edge-Driven Convection, shown by snapshots of potential temperature of various cases. (a) η_0 = 3.83·10^{18}. (b) η_0 = 1.96·10^{19}. (c) E_a = 120 kJ·mol^{-1}. (d) E_a = 300 kJ·mol^{-1}. (e) T_{ref} = 1300 °C. (f) T_{ref} = 1400 °C. All other parameters as in the reference case. White contours outline areas with active melting. Black contour refers to the isotherm of T = 1215 °C = 0.9·T_{ref}. Note that snapshots are chosen such that they show a similar stage of model evolution as in figure 3b (*i.e.*, mature EDC major downwelling), while model times differ due to the effects of rheological parameters on onset and vigor of EDC/SSC. Note Also note that the reference case (figure 3b,c) corresponds to an intermediate case for the trends shown in any of the rows: η_0 = 8.61·10^{18}; E_a = 200 kJ·mol^{-1}; T_{ref} = 1350 °C.

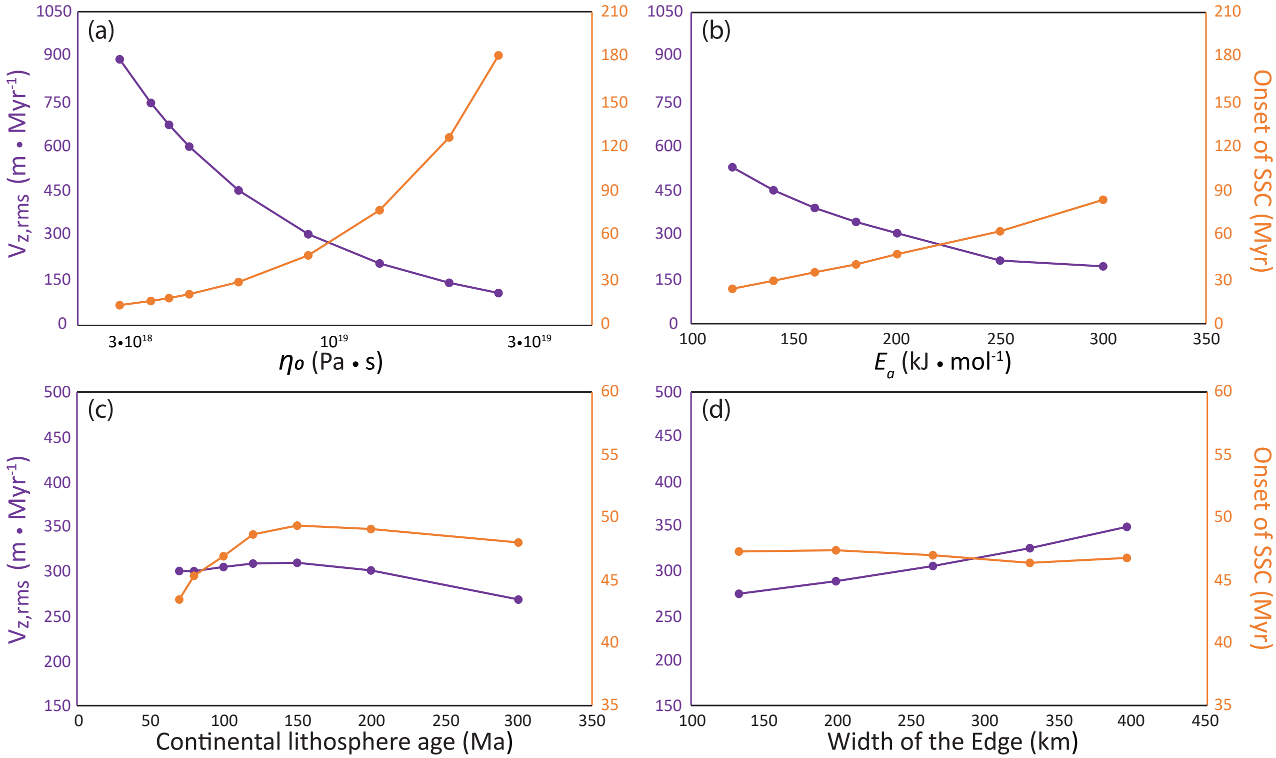

Figure 5. Diagrams showing the sensitivities of $v_{z,rms}$ (root mean square of vertical velocities) and of the onset age of small scale convection (starting from an oceanic crust of age 40 Ma) to selected parameters. (a) Reference viscosity (η_0). (b) Activation Energy (E_a). (c) Age (or thickness) of the continental lithosphere (τ_c). (d) Width in the horizontal direction of the edge (w). Note that the vertical axes of panels (c) and (d) are exaggerated with respect to those of panels (a) and (b).

EDC and, probably, due to SSC. This final thickness (*i.e.*, beneath old ocean basins) is constrained by seismic observations, and seafloor topography (Stein and Stein, 1994; Doin and Fleitout, 1996; van Hunen et al., 2005).

Figure 6b shows the compositional origin of the melts from figure 6a. In many of the models, only the pyroxenite component melts, if melting occurs at all. This prediction implies the formation of magmas that are extremely enriched. The enrichment tends to slightly decrease with increasing melt flux. The least enriched case is consistent with the highest volume in figure 6a, and corresponds to a model with E_a = 120 kJ·mol^{-1} and η_0 = 2.87 · 10^{18} Pa·s. Even in this extreme case, the melts are mostly pyroxenite-derived. Although the absolute numbers in figure 6b depend on the choices of our melting parameterizations and lithological assemblage (see section 2), the general trends will be similar as shown in figure 6b unless the pyroxenite component melts at a lower temperature than peridotite (Yaxley and Green, 1998; Shorttle et al., 2014; Lambart et al., 2016).

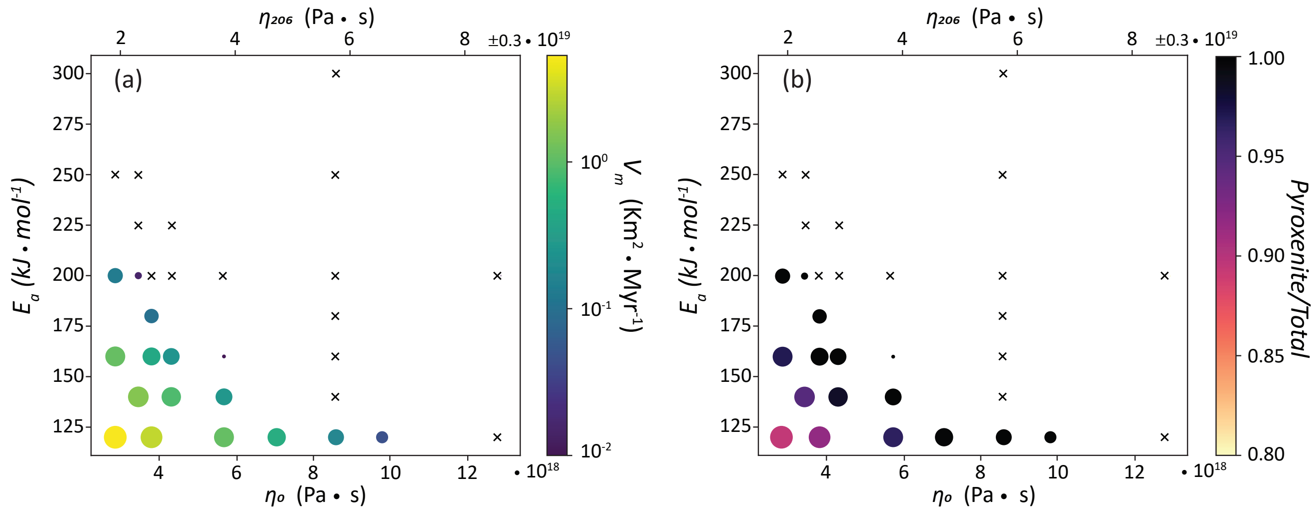

Figure 6. Scatter plots showing the melt properties variation with respect to the referent reference viscosity (η_0) and activation energy (E_a). The upper axis η_{206} refers to the viscosity in the asthenosphere measured at z = 206 km depth on the oceanic side for all cases with E_a = 200 kJ·mol^{-1}. For all other cases, this value slighly slightly varies according to (very small) temperature changes related to the half-space cooling model (see eq. 2), but by less than 5 %. (a) Melt volume flux due to EDC (colored circles), measured at the point of maximum EDC-related vertical velocitites (*i.e.*, $v_{z,rms}$). Crosses mark cases in which no melting is detected. The size of the circles also scale with melt volume fluxes. Melt volume fluxes are reported in km^2·Myr^{-1} due to the 2D character of the model (*i.e.* corresponding to km^3·Myr^{-1} per km of plate in the out-of-plane direction). (b) Scatter plot showing the origin of the melting products (*i.e.* proportion of melt derived from pyroxenite vs. total melt; colored circles). Notation of crosses and size of circles as in panel (a). Note that the color scale is set between 0.8 and 1 1.

3.3 Effects of lithospheric-edge geometry

Modification of τ_o within the small range explored here controls the convection patterns of EDC. We explore τ_o only in a small range ($30 \leq \tau_o \leq 50$ Ma) because any smaller τ_o yields melting at time t = 0, and any larger τ_o yields a metastable base of the lithosphere (*i.e.*, due to τ_o close to or larger than the onset age of SSC for η_0 in the reference case). With τ_o = 30 Ma, melting appears during the early stages of EDC but quickly ceases (at $t < 10$ Myrs), consistent with the results of the reference case (τ_o = 40 Ma). Reducing or increasing τ_o changes the convection patterns of EDC: decreasing the age (and hence initial thickness) of the oceanic lithosphere tends to promote more asymmetric downwellings. For η_0 as in the reference case, significant EDC-related melting requires $\tau_o \leq 30$ Ma. Widespread SSC (and related melting) is largely independent of τ_o.

Changing the continental thicknesses also modifies the patterns of convection. Figure 7 7 (a and b) shows that thicker continental lithospheres tend to increase the vigor of EDC, therefore augmenting the volume of related melting. However, this increase only occurs up to some point: for $\tau_c > 150$ Ma (figures 5c and 7b) the pattern of convection changes such that the maximum vertical velocity occurs at significantly greater depths than in the reference case (figure 3). As a result, the characteristic velocities of EDC slow down because the viscosity increases with depth (see eq. 2). The onset of SSC also decreases for $\tau_c > 150$ Ma. Similar to the effects of decreasing τ_o, increasing τ_c enhances the asymmetry of the EDC cell. This asymmetry, in turn, implies that less material from the base of the continental lithosphere, and more material from the base of the oceanic lithosphere is entrained by the EDC downwelling for higher τ_c.

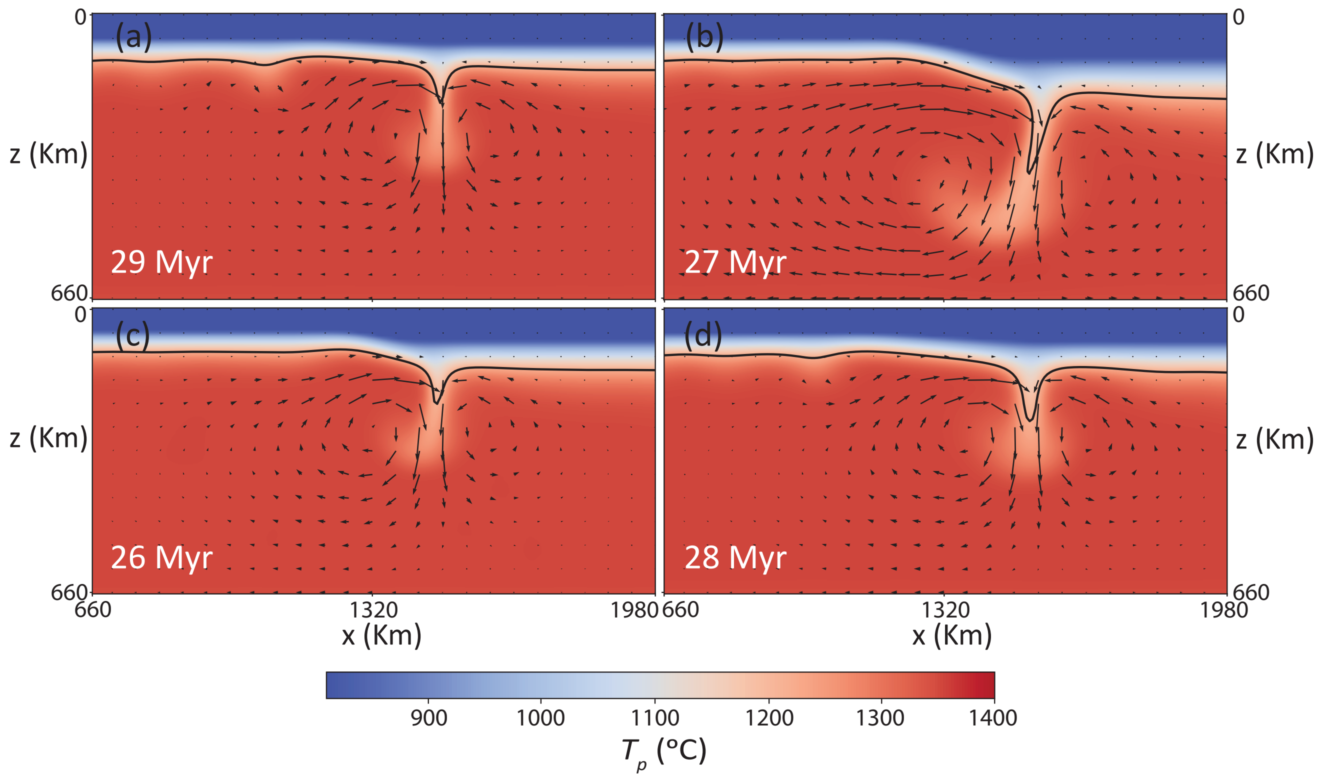

Figure 7. Effects of edge geometry on Edge-Driven Convection, shown by snapshots of potential temperature. (a) τ_c = 70 Ma. (b) τ_c = 150 Ma. (c) w = 132 km. (d) w = 396 km. All other parameters as in the reference case. Note that no melting occurs in any of the models. For clarity, note that the values of the reference case are τ_c = 100 Ma; w = 64 km.

Increasing w increases the $v_{z,rms}$ of EDC, probably due to more material from the lithosphere (thermal boundary layer) entrained in the downwelling(s) (figure 7d). Contrary to the previous cases, changing w does not affect noticeably the onset of SSC, which remains largely constant (figure 5d). These differences between changing τ_o and τ_c, and changing w, suggests that the geometrical effects cannot be simplified to an aspect-ratio-dependent parameter and that all geometrical parameters have a distinct effect.

Finally, we devise a model for the Canary Islands with τ_o = 40 Ma, w = 528 km, and a continental thermal age τ_c = 350 Ma (corresponding to a depth of 275 km for the 1215 °C isotherm), similar to consistent with the lithospheric thickness maps presented by Jessell et al. (2016, ; and references therein)Jessell et al. (2016, and references therein). Results from this model conform with the combined predictions of our cases with a very wide edge and with a very thick continental lithosphere ($v_{z,rms}$ = 287 m·Myr^{-1}, and onset of SSC = 48+40 Myr), suggesting that extrapolations from the trends in figure 5c,d are viable for settings outside the range of parameters systematically explored here. Also note that no melting was detected in this case.

3.4 Effects of internal heating

We also explore the effects of internal heating on model results. In principle, radioactive heating in the mantle should be much lower than that in the crust, but chemical heterogeneity may locally increase internal heating. We explore cases with increased internal heating everywhere, and others with increased internal heating just in the continental 'crust' (*i.e.*, yellow area in figure 2 with F = 1; as defined in section 2). We find that tripling the radiogenic heat production compared to the reference case everywhere has little influence on the vigor and geometry of EDC. However, it has an important influence on mantle melting, and also advances the onset of SSC which, then, becomes more vigorous than in the reference case (*i.e.*, with increased $v_{z,rms}$).

Increasing internal heating can induce melting, and boost the degrees and rates of melting, by limiting asthenospheric cooling. For example, as the mantle internal heating rate is unrealistically tripled in a model with activation energy E_a = 160 kJ·mol^{-1}, there is an increase in volcanism equivalent to reducing the E_a from 160 to 140 kJ·mol^{-1}, or to reducing η_0 from 8.61·10^{18} to 5.68·10^{18} Pa·s.

In nature, heat-producing elements tend to be concentrated in the continental crust due to their incompatible nature with respect to the mantle. We run an additional set of models with increased internal heating only in the continental crust H_c. Increasing the internal heating to $H_c = 5 \cdot H$ does not have any apparent effects on melting, nor it does affect the convection patters or $v_{z,rms}$. For $H_c = 10 \cdot H$, the average $v_{z,rms}$ is increased, but no substantial changes in terms of convection patterns are detected. Only for $H_c \geq 50 \cdot H$, significant changes occur compared to the reference case, with progressive lithospheric thinning on the continental side due to the effects of radioactive heating on the viscosity. At $H_c = 100 \cdot H$, melting occurs in the lower crust (followed by melting in the eroded continental lithosphere). In any case, $H_c \geq 50 \cdot H$ = 3.875·10^{-10} W·kg are unrealistic as an average value for the whole crustal thickness (Turcotte and Schubert, 2014).

3.5 Effects of volatile contents

Fluids released from the transition zone or other volatile-rich heterogeneities entrained by upper-mantle convection may also play an important role for intraplate volcanism, because they can greatly decrease melting temperatures. Unfortunately, dealing with amounts of water in a rock greater than the ones presented above remains a challenge for modeling (Green, 2015). We increase the water content in the enriched peridotitic component (EC) to 1000 ppm (0.1 %) in some models. In others, we also increase the abundance of EC (for from 15 % to 25 %). However, we emphasize that we are limited by the melting parameterization applied here (Katz et al., 2003), and hence are unable to explicitly model compositions that bear hydrous phases or other volatiles such as CO_2. In other words, H_2O concentrations in these additional models is a qualitative proxy for bulk volatiles in terms of their effects on melting behavior.

We find that for sufficiently large contents of H_2O in EC, EC melting starts to occur for the reference setting. The solidus of hydrous peridotite for 1000 ppm H_2O is below that of pyroxenite. In previous cases, pyroxenite was the main source (or even the sole one) of mantle melting. In this case the composition of magmas/melts is different than in previous cases and mostly peridotite-derived. In cases with high water contents in EC, melting is usually widespread, occurring due to EDC and SSC. Nonetheless, the amount of melting is very limited because of the low productivity of melting at low F in hydrous peridotite (Hirschmann et al., 1999; Katz et al., 2003; Asimow et al., 2004); and note that this productivity is much lower than that of the pyroxenite used here (Pertermann and Hirschmann, 2003). For example, the peak melt production in a case with 1000 ppm H2O H_2O in EC and a content of 25 % EC in the mantle assemblage is two orders of magnitude lower than that of the case with activation energy E_a = 120 kJ·mol^{-1} and η_0 = 2.87·10^{18} (*i.e.*, the case with maximum melt flux in figure 6).

3.6 Effects of plate motion

Another potentially important effect involves upper-mantle shear imposed by plate motion. All models presented above are stationary, *i.e.*, with v_{plate} = 0 cm·yr^{-1}, but on Earth plates move at finite speeds. Hence, we run additional models with an imposed plate velocity of 2, 4 and 6 cm·yr^{-1} in both directions perpendicular to the edge. Related shearing of the asthenosphere may contribute to melt production near the continent-ocean transition for plate motions in the direction of the continent (and hence opposite directions of mantle shear) due to shear-driven upwelling (King and Anderson, 1995, 1998; Conrad et al., 2010; Till et al., 2010). We find however that no melting is generated for plate velocities $\leq$ 6 cm·yr^{-1}, in models with a setting that otherwise conforms to the reference case.

4 Discussion

To explore the potential of EDC in terms of sustaining mantle melting and intraplate oceanic volcanism, we run a series of 2D convection models in a systematic parameter study. One robust result of our models involves the transient nature of EDC, with an evolving flow pattern and vigor. In all cases, EDC is followed by SSC, and EDC alone (*i.e.*, before the onset of widespread SSC) is never associated with high degrees or large volumes of mantle melting. In most models, EDC-related melting does not occur at all and, when it does, it is often short-lived and almost invariably followed by widespread melting due to SSC (except for the cases of T_{ref} = 1400 °C and τ_o = 30 Ma).

In all models in which melting due to EDC occurs, it happens soon after the beginning of the model and for only a short timespan. Keep in mind that EDC occurs mostly because the initial conditions of our models are metastable, and in reality should have started significantly earlier than time t = 0 Myr in our models, *e.g.*, immediately following rifting (van Wijk et al., 2010). Thus, any significant magmatism due to EDC beneath mature oceanic lithosphere is not realistic. On old lithosphere, if any melting occurs, it should occur widespread (due to SSC) and not localized (due to EDC). Pushing mantle properties to values that are more favorable for EDC-related melting invariably advances the onset of SSC (figure 5), therefore constraining even more the timing of purely EDC-related melting.

Although overall consistent (compare figure 6a with figure 6a of Kaislaniemi and Van Hunen, 2014), many of mour our results may strike as surprising when compared to previous work. In particular, our main conclusion of little-to-no melting due to EDC is in contrast to King and Anderson (1995, 1998), Till et al. (2010) and, to a smaller extent, Kaislaniemi and Van

Hunen (2014). To my our knowledge, no other work has self-consistently calculated the initial oceanic lithosphere depletion profile, and the initial condition indeed has a big influence on melting in these models, mostly due to the very transient nature of EDC. Indeed, a step-like edge can promote at least short-lived vigorous EDC and melting, but may not be realistic. This is not necessarily a criticism of previous work - for example, Kaislaniemi and Van Hunen (2014) deal with a tecton-craton transition in a continental setting - but rather a cautionary tale for future work regarding melting in the oceanic domain.

Kaislaniemi and Van Hunen (2014) suggested that increased radiogenic heating also used higher-than-realistic values for radiogenic heating to compensate for the potential lack of basal heating due to whole-mantle convection in regional-scale models. This increased heating may maintain otherwise transient EDC-related melting, and that this increased radiogenic heating may cause hotter temperatures beneath the continentsas well. My . However, our results suggest that increased higher-than-realistic internal heating can indeed have a significant effect on melting by itself, because it elevates mantle temperatures such that they exceed those for which the initial mid-ocean ridge depletion profile was calculated on the oceanic side (but note that in this case, the relevant origin of melting is not EDC anymore). Also, we find that strong enrichments of internal heat sources are required to have a significant effect on EDC-related melting . Although Furthermore, the lack of basal heating is not necessarily unrealistic because, for realistic rheologies, sub-adiabatic lower mantles have been inferred (*e.g.* Christensen and Yuen, 1985; Ulvrova et al., 2019). Indeed, EDC is a transient process and will be affected by re-heating of the upper mantle, but re-heating is achieved by other processes than those studied here (*e.g.* mantle wind or mantle plumes).

To stabilize the continental lithosphere, some authors have applied composition-dependent rheology (*e.g* King and Anderson, 1995; Kaislaniemi and Van Hunen, 2014). Such approach has the advantage of keeping the edge geometry mostly constant and being more suitable to study long-term processes. Unfortunately, there is no obvious and self-consistent way to calculate the lithological and rheological profile at the base of the continental lithosphere (see methods) and any proper analysis would hence require an extended parameter search. To explore the related first-order effects, we provide the result of a few additional models with compositional rheology switched on (Appendix B). We find that, even if the edge remains more stable, the process of EDC *sensu stricto* is still transient and the main conclusions remain robust. Moreover, the total amount of mantle melting due to EDC is smaller with rheological stabilization than without (for details, see Appendix B).

Another effect that emerges in models with rheological stabilization and radiogenic heating is a blanketing effect that may cause melting by processes other than EDC (see Appendix B). In reality, although a local enrichment of radiogenic elements, or a blanketing effect by a continent, is possible, Jain et al. (2019) showed recently that there is an inverse relation between increased radiogenic heating and the ability of continents to "heat" the mantle below "heat" the underlying mantle by isolation.

Till et al. (2010) were the first to systematically explore the effect of edge geometry in EDC flow. Their model setting was, however, different than ours, because they imposed a rheological stabilization of the craton and they focused on a setting with intense mantle wind. Under those conditions, mantle flow and melting change significantly because of shear-driven upwelling and decompression melting. My results overall agree with their study, nonetheless, except for predicting much lower melting volumes.

As demonstrated by our high-temperature models, EDC may (temporarily) sustain higher volume fluxes of melting, if hot materials are brought to the oceanic-continental transition for any reason. Such hot materials may be transported to the base of the lithosphere mainly by two processes: global mantle wind (*e.g.*, Behn et al., 2004; Conrad et al., 2011) flow related to whole mantle convection (*e.g.*, Behn et al., 2004; Conrad et al., 2011) or mantle plumes (for detailed investigation, see companion paper). Alternatively, the entrainment of hydrous or enriched materials by EDC may sustain moderate volcanism locally. For example, hydrous upwellings from the transition zone may be conveyed by EDC or SSC to the base of the lithosphere (Long et al., 2019). In this case, the underlying origin of mantle melting in the first place are the hydrous upwellings, and not EDC, even though the latter may ultimately control the geographic distribution of volcanism.

In any case, degrees of melting and related volume fluxes predicted by our models are unable to account for the high eruptions rates of the Canary Islands or Cape Verde (Hoernle and Schmincke, 1993; Carracedo et al., 1998; Plesner et al., 2003), even for a slow moving plate. We consider the case with greatest melt fluxes in figure 6a (E_a = 120 kJ·mol^{-1}; η_0 = 2.87·10^{18}): all magmas magma produced in the mantle before the onset of SSC-related melting will result in a 2D edifice of only 2.55 km height, assuming the most favorable conditions (no melt retention in the mantle, and complete extrusion to the surface) and an edifice slope of 18 degrees (Smith, 1988). This height is insufficient to explain emerged islands in the Canary archipelago, since the seafloor is $>$ 3 km below sea level. If we assume that 3D effects will focus melts into conical edifices with an spacing in the 3rd 3^{rd} dimension of 50 km (consistent with the separation of the islands La Palma and El Hierro), the height of the edifices would be 4.66 km above the sea floor, compatible with the height of small islands, such as El Hierro, but inadequate to explain the height of islands such as La Palma or Tenerife. These calculations demonstrate that not even this extreme case, with parameters that are marginally realistic for the Earth's mantle (E_a = 120 kJ·mol^{-1}; η_0 = 2.87·10^{18}), and considering favorable assumptions, can reproduce the volumes of major (subaerial) volcano chains such as the Canary Islands (or Cape Verde).

In addition, the short lifespan of EDC-related melting in models with low τ_o suggests that any related volcanism should occur on seafloor much younger than that underlying the Canaries or Cape Verde. Besides, no widespread magmatism such as due to SSC is observed in the vicinity of any of these archipelagos. Also, strictly-speaking, EDC melting is expected to sustain volcanism in an elongated zone that is parallel to the cratonic margin, and not localized like a hotspot. On the basis of the results of the models here presented, we draw the conclusion that Edge-Driven Convection alone is insufficient to sustain island-building volcanism near the African margin.

Furthermore, our models predict that EDC-related lavas invariable invariably originate from mantle melting of enriched lithologies such as pyroxenite (figure 6b). While volcanic compositions in the shield building stage of the Canaries are slightly more enriched than their Hawaiian counterparts (Abdel-Monem et al., 1971, 1972; Carracedo, 1999), they are not consistent with mostly pyroxenite-derived primary magmas. The models in which hydrous peridotite melts first - *i.e.*, the hydrous models - present even lower productivities and melting volumes. Geochemically speaking, we cannot favor and EDC origin for the main shield-building stage of the Canary or Cape Verde archipelagos either.

Nonetheless, there are some enriched volcanic compositions in the Eastern Atlantic, for example, the outcrops of carbonatites in the two archipelagos mentioned above (Allegre et al., 1971; Hoernle et al., 2002; Doucelance et al., 2010). Moreover, data about fluid inclusions in recent work suggests that current eruptions are among the most CO_2-rich for ocean islands (Taracsák et al., 2019, ; Esteban Gazel, Cornell University, personal communication, 2018)(Taracsák et al., 2019, Esteban Gazel, Cornell University, personal communication, 2018). Although it has been suggested that a high amount of CO_2 in the source is not required to explain the magmatic signatures of these islands (Schmidt and Weidendorfer, 2018), the influence of CO_2 on melting should not be ignored. Unfortunately, no efficient parameterization includes the effects of CO_2 on melting in the mantle in a way that we could incorporate it in our models. And the high water models of section 3.5 are only a proxy for what could happen.

While an alternative origin (such as a thermal anomaly) is required for the volcanic archipelagos, this does not imply that EDC does not happen near the western African margin. EDC occurs in all of my our models and must occur along every continental margin on Earth. Patriat and Labails (2006) found a “bulge” in the basement of the ocean-continent transition between the Canary Islands and Cape Verde. The location of this topographic anomaly coincides with the position of the main upwelling in our models (*i.e.*, at similar distances from the margin as predicted here). In turn, this “bulge” does not coincide with the inferred position of the Canary or Cape Verde hotspots.

In addition, Van Den Bogaard (2013) describes the formation of seamounts near the current position of, but significantly preceding, the Canary hotspot (Geldmacher et al., 2005). The timing and location of these seamounts is consistent with EDC-related melting beneath oceanic seafloor younger than 60 Ma, such as predicted by my our models (for example, the Bisabuelas seamount erupted 142 Ma ago in a much younger African Plate). Given my our model results, the geochemical signatures of these seamounts can be used as a test for their origin. We demonstrate that any EDC-related melting robustly implies strong geochemical enrichment.

One of the main conclusions of this study is the occurrence of EDC in absolutely all models run here, at least for a short duration. This is an intuitive result, as mantle convection is driven by lateral density differences. Even for a lithosphere that is intrinsically buoyant due to chemical anomalies, the thermal boundary layer will grow to the point where EDC starts (Lee et al., 2005). It is very likely that EDC starts as soon as rifting indents the lithosphere, resulting in an increased magmatism and erosion (King and Anderson, 1995; Sleep, 2007). Furthermore, although we have shown that EDC (by itself) is not a suitable mechanism for creating voluminous volcanic archipelagos, it could be responsible for smaller seamount provinces on young oceanic crust, such as the Canary Islands seamount province of Van Den Bogaard (2013).

Gerya et al. (2015) suggested that several processes during the history of the lithosphere may weaken it sufficiently to overcome the resistance to subduction initiation. In this sense, EDC-related low degree magmatism, although insufficient to generate archipelagos, may help to decrease the strength of the lithosphere in the continental-oceanic transition. This weakening could help to localize subduction zones along continental margins. The stresses related to EDC and SSC may further contribute to break plates (Solomatov, 2004; Mulyukova and Bercovici, 2018). We show that EDC can thermally erode and indent the lithosphere locally, and that melting will occur just below this indentation. Future work should focus on the role of EDC in subduction initiation.

Concerning limitations, my our models are intentionally simplified, because I we attempt to explore the systematic effects of rheological and geometrical parameters on Edge-Driven Convection and melting. We did not take into account effects like composition-dependent rheology or a rheologically stabilized craton. However, as the depleted and dehydrated lithosphere is expected to be more viscous than modeled here, our predicted velocities of EDC can be understood as upper bounds. Moreover, we show that erosion of the lithosphere is a prerequisite for EDC-related melting, and considering the effect of depletion stiffening will only reduce the degrees of melting and related volumes discussed in section 3. Lee et al. (2005) showed the importance of composition-dependent rheology for stabilizing cratons, and the influence of these variables on EDC needs to be better constrained. On the other hand, Currie and van Wijk (2016) showed that EDC and craton stability are intimately associated, and that the influence of EDC on craton formation and stability is poorly understood.

Finally, 3D models of EDC may present small differences with their 2D counterparts (Kaislaniemi and Van Hunen, 2014). We expect these discrepancies to be small, however, in particular for models with small plate velocities. For large plate velocities, the preferred geometry of SSC (longitudinal rolls; Richter and Parsons, 1975) is different than that prescribed in 2D models, and hence the onset age of SSC may be further advanced. In this sense, again, our model setup is conservative. Test models indeed confirm that key model predictions remain robust in 3D geometry.

5 Conclusions

In this paper, we study the formation of mantle melting and oceanic intraplate volcanism due to Edge-Driven Convection (EDC). As a complex, transient phenomenon, EDC is strongly affected by mantle rheological properties and the geometry of the base of the lithosphere. The following points summarize the key findings of this paper:

- Although EDC melting is not very vigorous, mantle flow due to EDC occurs for any combination of physical parameters realistic for the Earth, albeit it remains a transient phenomenon. We predict that EDC should occur everywhere on Earth where lateral density variations exist in the lithosphere, but is soon soon transition into widespread SSC.

- For a wide range of parameters, EDC is insufficient to sustain mantle melting at all. Only for a subset of the parameter space , (*e.g.*, for low E_a and/or low η_0), EDC can sustain magmatism. However, even for these models($e.g.$ low E_a and/or η_0), EDC-related magmatism can only build is rather weak and can only sustain the formation of small seamounts with very enriched geochemistry on young oceanic crust ($e.g.$ the Cretaceous-to-Paleogene Canary islands seamount province, Van Den Bogaard, 2013)(*e.g* the Cretaceous-to-Paleogene Canary islands seamount province).

- In turn, EDC is by far insufficient to sustain voluminous island-building volcanism, particularly on old seafloor (such as the Canaries or Cape Verde). On old seafloor, volcanism occurs is predicted by our models to occur widespread due to SSC, and not localized due to EDC (if it occurs at all).

- Although EDC melting is not very vigorous, mantle flow due to EDC occurs with any combination of physical parameters realistic for the Earth, albeit it remains a transient phenomenon. we predict that EDC should occur everywhere on Earth where lateral density variations exist in the lithosphere, but is soon joined by widespread SSC.

- Increased mantle temperatures or water contents can modify the vigor of convection and the amount of melting, but future work is needed to quantify the conditions under which such thermal/compositional anomalies can be sustained continuously in order to reproduce the large volumes of volcanism observed at the Eastern Atlantic Archipelagos.

A companion study citationdeals with the possible comprehensive (in prep.) will investigate the interaction between mantle plumes and Edge-Driven Convection.

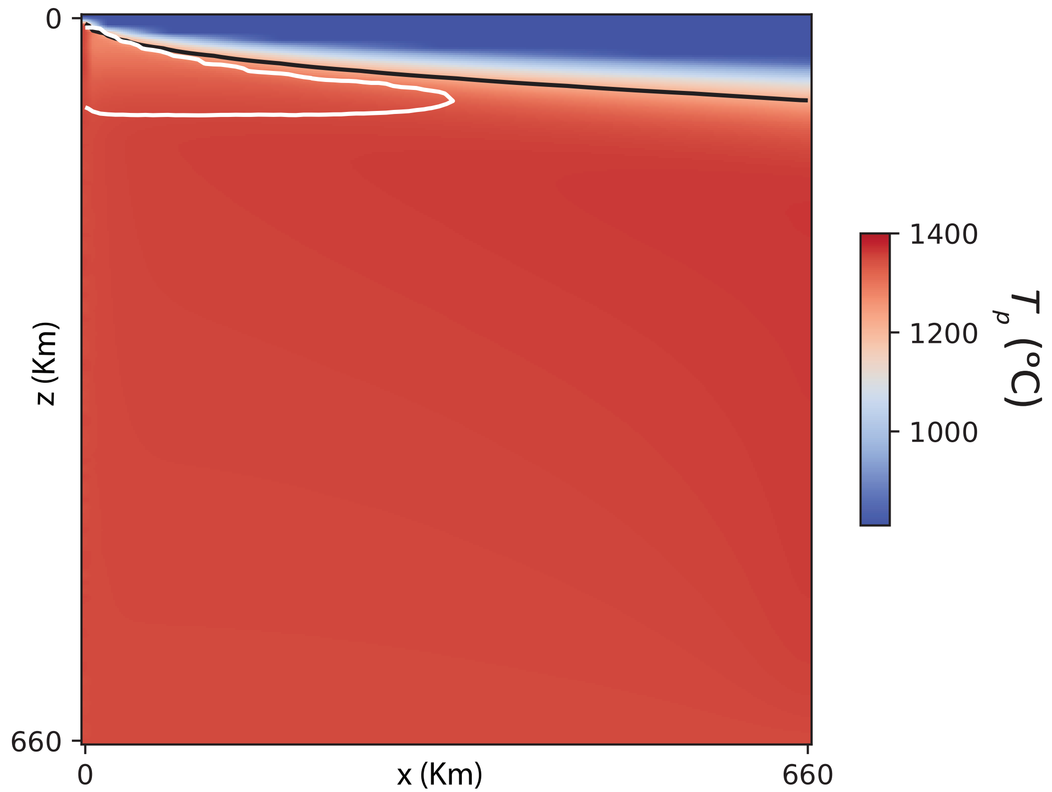

Figure A1. Temperature field and melting for an example mid-ocean ridge model (for description, see methods). For reference to contour lines, see figures 3 and 4 captions.

Code and data availability. The complete code and data used in this work are available upon request

Appendix A: Additional figures for the 'Methods' section

.

The following figures complement those presented in section 2. Figure A1 shows a snapshot of a corner flow model simulating flow and melting at a Mid-Ocean Ridge. these models are run to calculate the initial melt depletion profiles for the oceanic (and continental) lithosphere of the EDC models presented in the main text. Figure A2 shows the different compositional fields for a snapshot of the reference case. The most important feature of this figure is that the most enriched lithologies (EC and PX) are depleted also at the very base of the lithosphere. Erosion and removal of these enriched lithologies are crucial for melting in any models without significant thermal anomalies in the mantle (including our EDC models), and for which the depletion at the base of the lithosphere is self-consistently calculated.

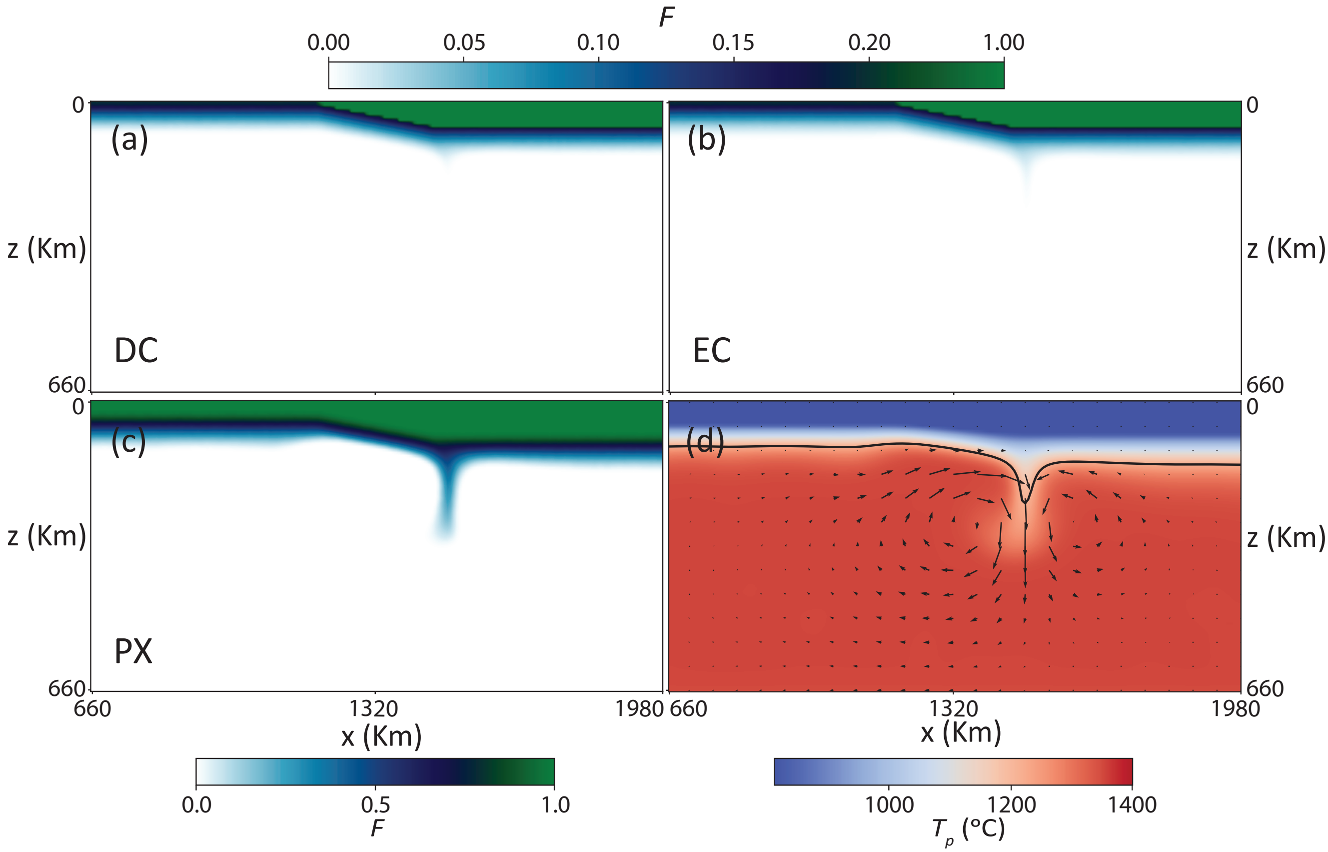

Figure A2. Snapshots of composition and temperature of the same timestep of the reference model as shown in figure 3b. Panels (a) and (b) show melt depletion the peridotitic compositions: DC and EC respectively. Panel (c) shows for the pyroxenitic (PX) component. Panel (d) is identical to figure 3b. Note that while peridotitic components are barely eroded and entrained by EDC, this is not true for the PX component. Also note that the scale for panel (c) is different than that of panels (a) and (b).

Appendix B: Extended discussion on rheological stabilization of continents and EDC

B1

To explore the effects of rheological stiffening and estabilization of the continental lithosphere, we run additional models of flow and melting with rheology-dependent viscosity. A priori, there is no indication that accounting for compositional rheology should strongly affect our results: a stiffer lithosphere is expected to promote less entrainment and erosion of the base of the lithosphere, which in turn should result in less melting. On the other hand composition-dependent rheology may help to maintain the edge, hence extending EDC-related flow.

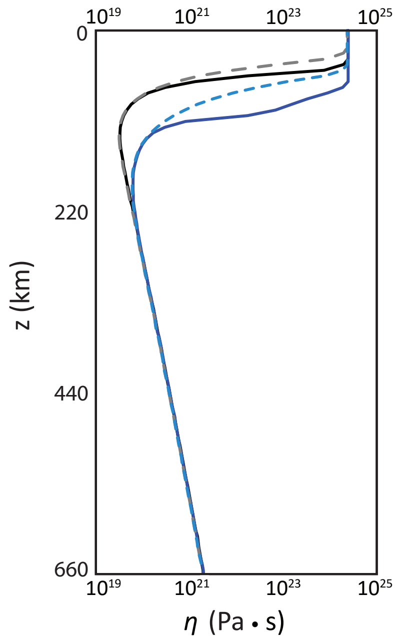

Figure B1. Viscosity profiles for cases with and without rheological stiffening. Solid lines correspond to cases with rheological stiffening, while dashed lines correspond to cases without. In black and grey, profile at the oceanic side of the model; in dark and light blue, profile at the continental side of the model. All the remaining properties as in the reference case.

We follow the rheological stiffening method of Ballmer et al. (2009), which calculates the increase in viscosity due to water loss in the main lithology (with increasing depletion of DC). We use a θ value of of 274.8, which corresponds to a viscosity contrast of a factor of 100 between the fully hydrated component and the dry component. This method relates stiffening with depletion as the material loses water during melting. Since the upper part of the continental lithosphere is simulated as an extremely depleted lid, this method leads to a greatly increased viscosity (*i.e.* a factor of 100) of the lithosphere on the continental side of the model. Consistently, significant stiffening also happens on the oceanic side, as the oceanic lithosphere is fully dehydrated at the top. For a comparison of viscosity profiles between the reference case of figure 3 and an equivalent case with rheological stiffening, see figure B1

Figure B2a shows a comparison of a model with rheological stabilization and one without. Indeed, they show similar characteristics, but the case with composition-dependent rheology shows less removal of the base of the lithosphere (figure B2b). Due to this less extensive removal, models with lithological stabilization produce lower melting volumes. For example, the models shown in figure B2 feature the same η_0 and E_a as the case with maximum melting in figure 6, but the case with compositional stiffening, displays lower volumes of melting than its counterpart without viscosity adjustment (*i.e.* 2.49 vs. 5.32 Km^2·Myr^{-1}).

The effect of lithological stiffening also emerges when analyzing the vigor of convection. Figure B3 shows different $v_{z,rms}$ for equivalent cases with and without composition-dependent rheology. As can be seen, the cases with compo-

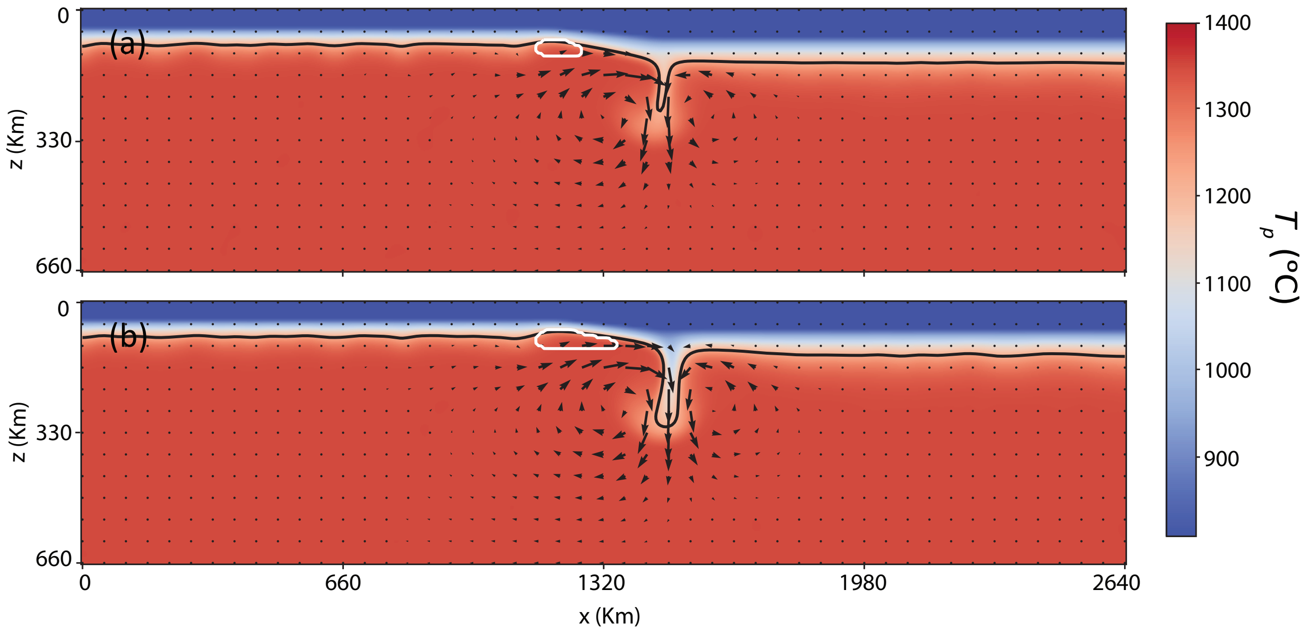

Figure B2. Model snapshots of mantle flow and melting for a case with composition-dependent rheology (panel a) and a case without composition-dependent rheology (panel b). Physical properties as in the case with maximum melting in figure 6 (η_0 = 2.87·10^{18} Pa·s; E_a = 120 kJ·mol^{-1}). Note that although the velocity fields are very similar, the case with rheological stabilization (panel a) shows less erosion at the base of the lithosphere than the case without (panel b), resulting in less vigorous upwellings and downwellings. Consequently, melting rates are also less important for the cases with composition-dependent rheology (compare the white contour of panel of panel a with that of panel b).

sitional rheology display systematically lower $v_{z,rms}$ than cases without. This result suggests that the melt volumes and vigor of EDC predicted by our models without compositional rheology (as presented in the main text) can be taken as upper bounds, therefore corroborating our conclusions.

Finally, our models do not predict that the duration of EDC and EDC-related melting would be significantly exteded for cases with compositional rheology and with stable continent and edge geometries (as suggested by Kaislaniemi and Van Hunen, 2014).

Author contributions. AMC performed the numerical experiments, as well as post-processed, analyzed and plotted the data. Both authors devised the study, interpreted the results, and wrote the paper.

Competing interests. The authors declare no competing interests.

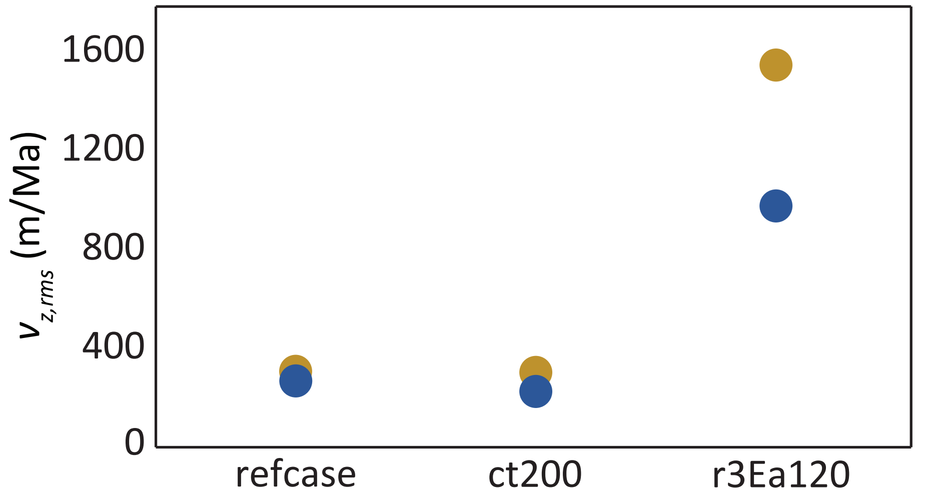

Figure B3. Diagram showing $v_{z,rms}$ for equivalent cases with (blue) and without (light brown) composition-dependent rheology. *refcase* corresponds to the reference case (see figure 3); *ct200* corresponds to a case with τ_c = 200 Ma; and *r3E120* corresponds to a case with η_0 = 2.87·10^{18} Pa·s and E_a = 120 kJ·mol^{-1} (*i.e.*, the case with maximum melting in figure 6). All other parameters as in the reference case (figure 3).

Acknowledgements. The Authors want to thank Prof. van Hunen and Dr. Rummel for their thorough reviews: the fruitful discussion that arose from them led to a significant improvement of this work. In addition, we want to thank Taras Gerya, Paul Tackley, Oliver Shorttle and Esteban Gazel for their insightful feedback on an earlier version of the paper. AMC has been supported by Swiss National Science Foundation grant 2-77026-16.

References

Abdel-Monem, A., Watkins, N. D., and Gast, P. W.: Potassium-Argon Ages, Volcanic Stratigraphy, and Geomagnetic Polarity History of the Canary Islands: Lanzatorte, Fuerteventura, Gran Canaria y La Gomera, American Journal of Science, 271, 490–521, http://www.ajsonline.org/content/271/5/490.full.pdf, 1971.

Abdel-Monem, A., Watkins, N. D., and Gast, P. W.: Potassium-Argon Ages, Volcanic Stratigraphy and Geomagnetic Polarity History of the Canary Islands: Tenerife, La Palma, and Hierro, American Journal of Science, 272, 805–825, http://www.ajsonline.org/content/272/9/805.full.pdf, 1972.

Allegre, C. J., Pineau, F., Bernat, M., and Javoy, M.: Evidence for the Occurrence of Carbonatites on the Cape Verde and Canary Islands, Nature, 233, 103–104, 1971.

Anderson, D. L.: Scoring hotspots: The plume and plate paradigms, in: Plates, plumes and paradigms: Geological Society of America Special Paper 388, edited by Foulger, G. R., Natland, J. H., Presnall, D. C., and Anderson, D. L., pp. 31–54, Geological Society of America, 2005.

Anguita, F. and Hernan, F.: The Canary Islands origin: a unifying model, Journal of Volcanology and Geothermal Research, 103, 1–26, www.elsevier.nl/locate/volgeores, 2000.

Araña, V. and Ortiz, R.: The Canary Islands: Tectonics, Magmatism and Geodynamic Framework, in: Magmatism in Extensional Structural Sttings, edited by Kampuzu, A. B. and Lubala, R. T., chap. 7, pp. 209–249, Springer - Verlag, 1991.

Asimow, P. D., Dixon, J. E., and Langmuir, C. H.: A hydrous melting and fractionation model for mid-ocean ridge basalts: Application to the Mid-Atlantic Ridge near the Azores, Geochemistry, Geophysics, Geosystems, 5, https://doi.org/10.1029/2003GC000568, 2004.

Ballmer, M. D.: Small-scale sublithospheric convection - an alternative mechanism for oceanic intraplate volcanism, Ph.D. thesis, ETH Zurich, 2009.

Ballmer, M. D.: Small-Scale Convection in the Earth's Mantle, in: Reference Module in Earth Systems and Environmental Sciences, Elsevier, https://doi.org/10.1016/b978-0-12-409548-9.09494-x, 2017.

Ballmer, M. D., van Hunen, J., Ito, G., Bianco, T. A., and Tackley, P. J.: Intraplate volcanism with complex age-distance patterns: A case for small-scale sublithospheric convection, Geochemistry, Geophysics, Geosystems, 10, https://doi.org/10.1029/2009GC002386, http://doi.wiley.com/10.1029/2009GC002386, 2009.

Ballmer, M. D., Conrad, C. P., Smith, E. I., and Harmon, N.: Non-hotspot volcano chains produced by migration of shear-driven upwelling toward the East Pacific Rise, Geology, 41, 479–482, https://doi.org/10.1130/G33804.1, 2013.

Ballmer, M. D., van Keken, P. E., and Ito, G.: Hotspots, Large Igneous Provinces, and Melting Anomalies, in: Treatise on Geophysics: Second Edition, edited by Schubert, G., vol. 7, pp. 393–459, Elsevier, https://doi.org/10.1016/B978-0-444-53802-4.00133-0, 2015.

Behn, M. D., Conrad, C. P., and Silver, P. G.: Detection of upper mantle flow associated with the African Superplume, Earth and Planetary Science Letters, 224, 259–274, https://doi.org/10.1016/j.epsl.2004.05.026, 2004.

Bodinier, J. L. and Godard, M.: Orogenic, Ophiolitic, and Abyssal Peridotites, in: Treatise on Geochemistry: Second Edition, vol. 3, pp. 103–167, Elsevier, https://doi.org/10.1016/B978-0-08-095975-7.00204-7, 2013.

Carracedo, J. C.: Growth, structure, instability and collapse of Canarian volcanoes and comparisons with Hawaiian volcanoes, Journal of Volcanology and Geothermal Research, 94, 1–19, www.elsevier.comrlocaterjvolgeores, 1999.

Carracedo, J. C., Day, S., Guillou, H., Rodríguez Badiola, E., Canas, J. A., and Pérez Torrado, F. J.: Hotspot volcanism close to a passive continental margin: the Canary Islands, Geological Magazine, 135, 591–604, https://www.cambridge.org/core/journals/geological-magazine/

article/hotspot-volcanism-close-to-a-passive-continental-margin-the-canary-islands/26D6FD3C9CA2DAC201366C987DBAFC31, 1998.

Christensen, U. R.: Convection with pressure- and temperature-dependent non-Newtonian rheology, Geophysical Journal of the Royal Astronomical Society, 77, 343–384, https://doi.org/10.1111/j.1365-246X.1984.tb01939.x, https://academic.oup.com/gji/article-lookup/doi/10.1111/j.1365-246X.1984.tb01939.x, 1984.

Christensen, U. R. and Yuen, D. A.: Layered convection induced by phase transitions, Journal of Geophysical Research, 90, 10 291, https://doi.org/10.1029/JB090iB12p10291, http://doi.wiley.com/10.1029/JB090iB12p10291, 1985.

Conrad, C. P., Wu, B., Smith, E. I., Bianco, T. A., and Tibbetts, A.: Shear-driven upwelling induced by lateral viscosity variations and asthenospheric shear: A mechanism for intraplate volcanism, Physics of the Earth and Planetary Interiors, 178, 162–175, https://doi.org/10.1016/J.PEPI.2009.10.001, https://www.sciencedirect.com/science/article/pii/S003192010900209X?via{%}3Dihub, 2010.

Conrad, C. P., Bianco, T. A., Smith, E. I., and Wessel, P.: Patterns of intraplate volcanism controlled by asthenospheric shear, Nature Geoscience, https://doi.org/10.1038/ngeo1111, 2011.

Courtillot, V., Davaille, A., Besse, J., and Stock, J.: Three distinct types of hotspots in the Earth's mantle, Earth and Planetary Science Letters, 205, 295–308, https://doi.org/10.1016/S0012-821X(02)01048-8, 2003.

Currie, C. A. and van Wijk, J.: How craton margins are preserved: Insights from geodynamic models, Journal of Geodynamics, 100, 144–158, https://doi.org/10.1016/J.JOG.2016.03.015, https://www.sciencedirect.com/science/article/pii/S0264370716300552, 2016.

Doblas, M., López-Ruiz, J., and Cebriá, J. M.: Cenozoic evolution of the Alboran Domain: A review of the tectonomagmatic models, https://doi.org/10.1130/2007.2418(15), 2007.

Doin, M. and Fleitout, L.: Thermal evolution of the oceanic lithosphere: an alternative view, Earth and Planetary Science Letters, 142, 121–136, https://doi.org/10.1016/0012-821X(96)00082-9, https://www.sciencedirect.com/science/article/pii/0012821X96000829, 1996.

Doucelance, R., Hammouda, T., Moreira, M., and Martins, J. C.: Geochemical constraints on depth of origin of oceanic carbonatites: The Cape Verde case, Geochimica et Cosmochimica Acta, 74, 7261–7282, https://doi.org/10.1016/j.gca.2010.09.024, 2010.

Dumoulin, C., Doin, M. P., Arcay, D., and Fleitout, L.: Onset of small-scale instabilities at the base of the lithosphere: Scaling laws and role of pre-existing lithospheric structures, Geophysical Journal International, 160, 345–357, https://doi.org/10.1111/j.1365-246X.2004.02475.x, 2005.

Foulger, G. and Anderson, D. L.: A cool model for the Iceland hotspot, Journal of Volcanology and Geothermal Research, 141, 1–22, https://doi.org/10.1016/j.jvolgeores.2004.10.007, 2005.

Geldmacher, J., Hoernle, K. A., Bogaard, D., Duggen, S., and Werner, R.: New 40Ar39Ar age and geochemical data from seamounts in the Canary and Madeira volcanic provinces: Support for the mantle plume hypothesis, Earth and Planetary Science Letters, 237, 85–101, https://doi.org/10.1016/j.epsl.2005.04.037, https://ac.els-cdn.com/S0012821X05002876/1-s2.0-S0012821X05002876-main.pdf?{_}tid=f50d537f-5f7c-4190-8a21-2e63603d17a8{&}acdnat=1530783938{_}f1f5a63e4d80a645df85afdfaa7d8891, 2005.

Gerya, T. V., Stern, R. J., Baes, M., Sobolev, S. V., and Whattam, S. A.: Plate tectonics on the Earth triggered by plume-induced subduction initiation, Nature, 527, 221–225, https://doi.org/10.1038/nature15752, http://www.nature.com/articles/nature15752, 2015.

Green, D. H.: Experimental petrology of peridotites, including effects of water and carbon on melting in the Earth's upper mantle, Physics and Chemistry of Minerals, 42, 95–122, https://doi.org/10.1007/s00269-014-0729-2, http://link.springer.com/10.1007/s00269-014-0729-2, 2015.

Hirano, N.: Petit-spot volcanism: A new type of volcanic zone, Geochemical Journal, 45, 157–167, https://doi.org/10.2343/geochemj.1.0111, 2011.

Hirschmann, M. M.: Mantle solidus: Experimental constraints and the effects of peridotite composition, Geochemistry, Geophysics, Geosystems, 1, https://doi.org/10.1029/2000GC000070, http://doi.wiley.com/10.1029/2000GC000070, 2000.

Hirschmann, M. M. and Stolper, E. M.: A possible role for garnet pyroxenite in the origin of the "garnet signature" in MORB, Contributions to Mineralogy and Petrology, 124, 185–208, https://doi.org/10.1007/s004100050184, http://link.springer.com/10.1007/s004100050184, 1996.

Hirschmann, M. M., Asimow, P. D., Ghiorso, M. S., and Stolper, E. M.: Calculation of peridotite partial melting from thermodynamic models of minerals and melts. III. Controls on Isobaric Melt Production and the Effect of Water on Melt Production., Journal of Petrology, 40, 831–851, http://petrology.oxfordjournals.org/, 1999.

Hirth, G. and Kohlstedt, D. L.: Water in the oceanic upper mantle: implications for rheology, melt extraction and the evolution of the lithosphere, Earth and Planetary Science Letters, 144, 93–108, https://doi.org/10.1016/0012-821X(96)00154-9, 1996.

Hoernle, K. and Schmincke, H.-U.: The Role of Partial Melting in the 15-Ma Geochemical Evolution of Gran Canada: A Blob Model for the Canary Hotspot, Journal of Petrology, 34, 599–629, https://academic.oup.com/petrology/article-abstract/34/3/599/1421890, 1993.

Hoernle, K., Tilton, G., Le Bas, M. J., Duggen, S., and Garbe-Schönberg, D.: Geochemistry of oceanic carbonatites compared with continental carbonatites: Mantle recycling of oceanic crustal carbonate, Contributions to Mineralogy and Petrology, 142, 520–542, https://doi.org/10.1007/s004100100308, 2002.

Huang, J., Zhong, S. J., and van Hunen, J.: Controls on sublithospheric small-scale convection, Journal of Geophysical Research, 108, https://doi.org/10.1029/2003jb002456, 2003.

Iwamori, H., McKenzie, D., and Takahashi, E.: Melt generation by isentropic mantle upwelling, Earth and Planetary Science Letters, 134, 253–266, https://doi.org/10.1016/0012-821X(95)00122-S, https://linkinghub.elsevier.com/retrieve/pii/0012821X9500122S, 1995.

Jain, C., Rozel, A. B., Tackley, P. J., Sanan, P., and Gerya, T. V.: Growing primordial continental crust self-consistently in global mantle convection models, Gondwana Research, 73, 96–122, https://doi.org/10.1016/J.GR.2019.03.015, https://www.sciencedirect.com/science/article/pii/S1342937X19301066, 2019.

Jessell, M. W., Begg, G. C., and Miller, M. S.: The geophysical signatures of the West African Craton, Precambrian Research, 274, 3–24, https://doi.org/10.1016/j.precamres.2015.08.010, 2016.

Kaislaniemi, L. and Van Hunen, J.: Dynamics of lithospheric thinning and mantle melting by edge-driven convection: Application to Moroccan Atlas mountains, Geochemistry, Geophysics, Geosystems, 15, 3175–3189, https://doi.org/10.1002/2014GC005414, 2014.

Karato, S.-i. and Wu, P.: Rheology of the Upper Mantle: A Synthesis, Science, 260, 771–778, 1993.

Katz, R. F., Spiegelman, M., and Langmuir, C. H.: A new parameterization of hydrous mantle melting, Geochemstry, Geophysics, Geosystems, 4, https://doi.org/10.1029/2002GC000433, https://agupubs.onlinelibrary.wiley.com/doi/pdf/10.1029/2002GC000433, 2003.

King, S. D. and Adam, C.: Hotspot swells revisited, Physics of the Earth and Planetary Interiors, 235, 66–83, https://doi.org/10.1016/j.pepi.2014.07.006, 2014.

King, S. D. and Anderson, D. L.: An alternative mechanism of flood basalt formation, Earth and Planetary Science Letters, 136, 269–279, https://doi.org/10.1016/0012-821X(95)00205-Q, 1995.

King, S. D. and Anderson, D. L.: Edge-driven convection, Earth and Planetary Science Letters, 160, 289–296, https://doi.org/10.1016/S0012-821X(98)00089-2, 1998.

King, S. D. and Ritsema, J.: African Hot Spot Volcanism: Small-Scale Convection in the Upper Mantle Beneath Cratons, Science, 290, 1137–1139, http://science.sciencemag.org/, 2000.

Lambart, S., Baker, M. B., and Stolper, E. M.: The role of pyroxenite in basalt genesis: Melt-PX, a melting parameterization for mantle pyroxenites between 0.9 and 5 GPa, Journal of Geophysical Research: Solid Earth, 121, 5708–5735, https://doi.org/10.1002/2015JB012762, https://onlinelibrary.wiley.com/doi/abs/10.1002/2015JB012762, 2016.

Lee, C.-T. A., Lenardic, A., Cooper, C. M., Niu, F., and Levander, A.: The role of chemical boundary layers in regulating the thickness of continental and oceanic thermal boundary layers, Earth and Planetary Science Letters, 230, 379–395, https://doi.org/10.1016/j.epsl.2004.11.019, https://linkinghub.elsevier.com/retrieve/pii/S0012821X04007022, 2005.

Long, X., Ballmer, M. D., Manjón-Cabeza Córdoba, A., and Li, C. F.: Mantle Melting and Intraplate Volcanism Due to Self-Buoyant Hydrous Upwellings From the Stagnant Slab That Are Conveyed by Small-Scale Convection, Geochemistry, Geophysics, Geosystems, 20, 4972–4997, https://doi.org/10.1029/2019GC008591, 2019.

Martinez-Arevalo, C., Mancilla, F. d. L., Helffrich, G., and Garcia, A.: Seismic evidence of a regional sublithospheric low velocity layer beneath the Canary Islands, Tectonophysics, 608, 586–599, https://doi.org/10.1016/j.tecto.2013.08.021, 2013.

McKenzie, D. and Bickle, M. J.: The Volume and Composition of Melt Generated by Extension of the Lithosphere, Journal of Petrology, 29, 625–679, 1989.

Moresi, L. N. and Gurnis, M.: Constraints on the lateral strength of slabs from three-dimensional dynamic flow models, Earth and Planetary Science Letters, 138, 15–28, https://doi.org/10.1016/0012-821X(95)00221-W, 1996.

Moresi, L. N. and Solomatov, V. S.: Numerical investigation of 2D convection with extremely large viscosity variations, Physics of Fluids, 7, 2154–2162, https://doi.org/10.1063/1.868465, 1995.

Morgan, W. J.: Convection Plumes in the Lower Mantle, Nature, 230, 42–43, https://doi.org/10.1038/230042a0, 1971.

Mulyukova, E. and Bercovici, D.: Collapse of passive margins by lithospheric damage and plunging grain size, Earth and Planetary Science Letters, 484, 341–352, https://doi.org/10.1016/j.epsl.2017.12.022, www.elsevier.com/locate/epsl, 2018.

Parsons, B. and McKenzie, D.: Mantle convection and the thermal structure of the plates, Journal of Geophysical Research, 83, 4485, https://doi.org/10.1029/jb083ib09p04485, 1978.

Patriat, M. and Labails, C.: Linking the Canary and Cape-Verde Hot-Spots, Northwest Africa, Marine Geophysical Researches, 27, 201–215, https://doi.org/10.1007/s11001-006-9000-7, http://link.springer.com/10.1007/s11001-006-9000-7, 2006.

Pertermann, M. and Hirschmann, M. M.: Anhydrous Partial Melting Experiments on MORB-like Eclogite: Phase Relations, Phase Compositions and Mineral-Melt Partitioning of Major Elements at 2-3 GPa, Journal of Petrology, 44, 2173–2201, https://doi.org/10.1093/petrology/egg074, 2003.

Plesner, S., Holm, P. M., and Wilson, J. R.: 40-39Ar geochronology of Santo Antão, Cape Verde Islands, Journal of Volcanology and Geothermal Research, 120, 103–121, https://doi.org/10.1016/S0377-0273(02)00367-0, www.elsevier.com/locate/jvolgeores, 2003.

Richter, F. M.: Convection and the large-scale circulation of the mantle, Journal of Geophysical Research, 78, 8735–8745, https://doi.org/10.1029/jb078i035p08735, 1973.

Richter, F. M. and Parsons, B.: On the interaction of two scales of convection in the mantle, Journal of Geophysical Research, 80, 2529–2541, https://doi.org/10.1029/jb080i017p02529, 1975.

Sacek, V.: Post-rift influence of small-scale convection on the landscape evolution at divergent continental margins, Earth and Planetary Science Letters, 459, 48–57, https://doi.org/10.1016/j.epsl.2016.11.026, 2017.

Sandwell, D. T., Winterer, E. L., Mammerickx, J., Duncan, R. A., Lynch, M. A., Levitt, D. A., and Johnson, C. L.: Evidence for diffuse extension of the Pacific Plate from Pukapuka ridges and cross-grain gravity lineations, Journal of Geophysical Research: Solid Earth, 100, 15 087–15 099, https://doi.org/10.1029/95JB00156, 1995.

Schmidt, M. W. and Weidendorfer, D.: Carbonatites in oceanic hotspots, Geology, 46, 435–438, https://doi.org/10.1130/G39621.1, https://gsw.silverchair-cdn.com/gsw/Content{_}public/Journal/geology/46/5/10.1130{_}G39621.1/2/435.pdf?Expires=1527179673{&}Signature=0JeMXRP5sW3Z2SQ7vk7Ja7jullOBZngHBLHqltL-hYwKa96-7UiqGkAg01mxsj96cBGvR0zigT6576oeDXDZy6oRo7k 2018.

Schutt, D. L. and Lesher, C. E.: Effects of melt depletion on the density and seismic velocity of garnet and spinel lherzolite, Journal of Geophysical Research: Solid Earth, 111, https://doi.org/10.1029/2003JB002950, http://doi.wiley.com/10.1029/2003JB002950, 2006.

Shorttle, O., Maclennan, J., and Lambart, S.: Quantifying lithological variability in the mantle, Earth and Planetary Science Letters, 395, 24–40, https://doi.org/10.1016/j.epsl.2014.03.040, www.elsevier.com/locate/epslhttp://creativecommons.org/licenses/by/3.0/, 2014.

Sleep, N. H.: Edge-modulated stagnant-lid convection and volcanic passive margins, Geochemistry, Geophysics, Geosystems, 8, n/a–n/a, https://doi.org/10.1029/2007GC001672, http://doi.wiley.com/10.1029/2007GC001672, 2007.

Smith, D. K.: Shape analysis of Pacific seamounts, Earth and Planetary Science Letters, 90, 457–466, https://doi.org/10.1016/0012-821X(88)90143-4, https://linkinghub.elsevier.com/retrieve/pii/0012821X88901434, 1988.

Solomatov, V. S.: Initiation of subduction by small-scale convection, Journal of Geophysical Research: Solid Earth, 109, https://doi.org/10.1029/2003jb002628, http://doi.wiley.com/10.1029/2003JB002628, 2004.

Stein, C. A. and Stein, S.: Constraints on hydrothermal heat flux through the oceanic lithosphere from global heat flow, Journal of Geophysical Research: Solid Earth, 99, 3081–3095, https://doi.org/10.1029/93JB02222@10.1002/(ISSN)2169-9356.OCRUST1, https://agupubs.onlinelibrary.wiley.com/doi/abs/10.1029/93JB02222{%}4010.1002/{%}28ISSN{%}292169-9356.OCRUST1, 1994.

Taracsák, Z., Hartley, M., Burgess, R., Edmonds, M., Iddon, F., and Longpré, M.-A.: High fluxes of deep volatiles from ocean island volcanoes: Insights from El Hierro, Canary Islands, Geochimica et Cosmochimica Acta, 258, 19–36, https://doi.org/10.1016/J.GCA.2019.05.020, https://www.sciencedirect.com/science/article/pii/S001670371930287X?via{%}3Dihub, 2019.

Thirlwall, M. F., Singer, B. S., and Marriner, G. F.: ^{3}9Ar ^{4}0Ar ages and geochemistry of the basaltic shield stage of Tenerife, Canary Islands, Spain, Journal of Volcanology and Geothermal Research, 103, 247–297, www.elsevier.nl/locate/jvolgeores, 2000.

Till, C. B., Elkins-Tanton, L. T., and Fischer, K. M.: A mechanism for low-extent melts at the lithosphere-asthenosphere boundary, Geochemistry, Geophysics, Geosystems, https://doi.org/10.1029/2010GC003234, 2010.

Turcotte, D. and Schubert, G.: Geodynamics, Cambridge University Press, Cambridge (UK), 3rd edn., 2014.

Ulvrova, M. M., Coltice, N., Williams, S., and Tackley, P. J.: Where does subduction initiate and cease? A global scale perspective, Earth and Planetary Science Letters, 528, https://doi.org/10.1016/j.epsl.2019.115836, https://doi.org/10.1016/j.epsl.2019.115836https://linkinghub.elsevier.com/retrieve/pii/S0012821X1930528X, 2019.

Van Den Bogaard, P.: The origin of the Canary Island Seamount Province -New ages of old seamounts, Scientific Reports, 3, 7, https://doi.org/10.1038/srep02107, https://www.nature.com/articles/srep02107.pdf, 2013.

van Hunen, J., Zhong, S., Shapiro, N. M., and Ritzwoller, M. H.: New evidence for dislocation creep from 3-D geodynamic modeling of the Pacific upper mantle structure, Earth and Planetary Science Letters, 238, 146–155, https://doi.org/10.1016/J.EPSL.2005.07.006, https://www.sciencedirect.com/science/article/pii/S0012821X05004619, 2005.

van Wijk, J. W., van Hunen, J., and Goes, S.: Small-scale convection during continental rifting: Evidence from the Rio Grande rift, Geology, 36, 575–578, https://doi.org/10.1130/G24691A.1, 2008.

van Wijk, J. W., Baldridge, W. S., van Hunen, J., Goes, S., Aster, R., Coblentz, D. D., Grand, S. P., and Ni, J.: Small-scale convection at the edge of the Colorado Plateau: Implications for topography, magmatism, and evolution of Proterozoic lithosphere, Geology, 38, 611–614, https://doi.org/10.1130/G31031.1, 2010.

Vogt, P. R.: Bermuda and Appalachian-Labrador rises: Common non-hotspot processes?, Geology, 19, 41, https://doi.org/10.1130/0091-7613(1991)019<0041:BAALRC>2.3.CO;2, https://pubs.geoscienceworld.org/geology/article/19/1/41-44/205166, 1991.

Wilson, J. T.: A Possible Origin of the Hawaiian Islands, Canadian Journal of Physics, 41, 863–870, https://doi.org/10.1139/p63-094, 1963.

Yaxley, G. M. and Green, D. H.: Reactions between eclogite and peridotite: mantle refertilisation by subduction of oceanic crust, schweizer mineralogische und petrographische Mitteilungen, 78, 243–255, 1998.

Zhong, S. J., Zuber, M. T., Moresi, L. N., and Gurnis, M.: Role of temperature-dependent viscosity and surface plates in spherical shell models of mantle convection, Journal of Geophysical Research: Solid Earth, 105, 11 063–11 082, https://doi.org/10.1029/2000JB900003, http://doi.wiley.com/10.1029/2000JB900003, 2000.